Online Learning of Gait Models

by

Jamie L. S. Waugh

A thesis
presented to the University of Waterloo
in fulfillment of the
thesis requirement for the degree of
Master of Applied Science
in
Electrical and Computer Engineering

Waterloo, Ontario, Canada, 2018

I hereby declare that I am the sole author of this thesis. This is a true copy of the thesis, including any required final revisions, as accepted by my examiners.

I understand that my thesis may be made electronically available to the public.

Abstract

Gait event identification is the identification of gait events (*e.g.*, foot impact) which occur cyclically, at the same location in each gait cycle. Gait event identification plays an important role in many applications, such as health monitoring, diagnosis, and rehabilitation. The majority of gait event identification algorithms are based on heuristics, many of which are threshold-based, making them sensitive to threshold parameters and causing poor generalization to new data (*e.g.*, different gait type, ground surface, sensor placement, footwear, etc.). While a number of machine learning techniques have been proposed, they use offline training and do not generalize well to data that is different from the training set.

This thesis proposes a novel approach for online, individualized gait analysis, based on an adaptive periodic model of any gait signal. The proposed method learns a model of the gait cycle during online measurement, using a continuous representation that can adapt to inter and intra-personal variability by creating an individualized model. The model of gait is learned online during observation, using incremental updates to the model parameters based on the error between the model-predicted and measured signal. The gait data is modeled as a periodic signal with a continuous phase variable, allowing data to be automatically labeled with a phase value corresponding to a particular event that re-occurs each gait cycle. Once the algorithm has converged to the input signal, key gait events can be identified based on the estimated gait phase.

Two methods of gait event identification were implemented: analytical event identification and initial event identification. Since we learn a gait model that has an analytical representation, if we know the properties of the gait events of interest, we can use the model to directly compute the corresponding phase. For example, to identify the peak event in each gait cycle, we can solve for the phase which generates the maximum value and assign this as the peak phase value. In the initial event identification method, we provide a manual or heuristic identification of a gait event in the first converged gait cycle and use the corresponding event phase to identify all future events. Once gait events are identified relative to the estimated gait phase, we can automatically identify any future events since we assume they occur at the same phase, as is common in gait analysis.

Our approach is implemented and tested on two datasets: one measuring mediolateral angular velocity of the ankles from a healthy young group of adults and the other measuring sagittal linear acceleration of the ankles from a group of retirement home residents who each have a variety of medical conditions. For the former dataset, the proposed approach converges within approximately five gait cycles and heel impact and toe takeoff events

are extracted with an average error of 0.04 gait cycles, using the manual initial event identification method.

For the latter dataset, the proposed approach converges within approximately eight gait cycles and initial swing events are extracted with an average error of 0.03 gait cycles, using the analytical event identification method. When using learning rates optimized on a set of training trials (opposed to a default set of learning rates), the proposed approach converges within approximately four gait cycles and maintains an average error of 0.03 gait cycles, on the corresponding set of test trials. Further, when including ground truth events occurring prior to the model having met convergence criteria, the average error is only slightly increased to 0.04 gait cycles.

Acknowledgements

I would like to thank my supervisor, Dana Kulić, for providing me with exciting opportunities, helpful advice, support, and countless edits, feedback, and brilliant ideas. Her high expectations, dedication to students, and contagious passion make for an exemplary supervisor who continues to inspire me.

This thesis would not have been possible without the collaboration of the Neuroscience, Mobility and Balance (NiMbAL) lab in the Kinesiology department at the University of Waterloo; in particular, the help of Anton Trinh, Julia E. Fraser, Kit B. Beyer, Ryan R. Mohammed, and William E. McIlroy. The NiMbAL lab collected both datasets: the young adult dataset from students at the university and the older adult dataset from retirement communities across Ontario, Canada. Gaining their insight was invaluable to this work. In particular, I would like to thank: Anton for his continued help, persistence, and our many discussions; Julia for her constant support, advice, and dedication to the progress of this research; and Kit for his hard work debugging the LabVIEW program used for ground truth event identification of the older adult dataset.

Elaine Huang did a thorough job, manually labelling gait events in the older adult dataset, and contributed a significant amount of time toward this research.

Thanks to my readers, James Tung and Allaa Hilal, for reviewing and providing feedback on this thesis.

I am grateful for my friends and colleagues, Adam Gomes, Keegan Fernandes, Ryan MacDonald, and Stanislav Bochkarev, for offering much of their time to brainstorm and solve problems to my liking and being a constant source of support.

Many thanks to all members of the Adaptive Systems Lab for being generous with their help and teaching me about many new topics over the years. Special thanks to Vladimir Joukov, Jonathan Lin, Terry Taewoong Um, Brandon J. DeHart, Rezvan Kianifar, Alexandru Blidaru, and Kevin Westermann for their advice and help throughout my degree.

I would like to thank everyone in the Larsen group at Inria - Nancy Grand Est for their help with my work there, especially Serena Ivaldi and Olivier Rochel.

Finally, I would like to thank my family and friends for their constant support and encouragement throughout my life. Throughout my degree in particular, I would like to thank Lloyd Waugh, Maryhelen Stevenson, Adam Gomes, Takin Tadayon, Angela Herring-Lauzon, Ritika Kalia, Lilly Zheng, Emily Nickerson, Eric Bouchard, Ryan MacDonald, Chris Sanichar, Roberto Alejandro Rama Vilariño, Vaios Papaspyros, and Charles Waugh.

This research was partially funded by the Ontario Graduate Scholarship Program and Mitacs, and was made possible by the facilities of the Shared Hierarchical Academic Research Computing Network (SHARCNET:www.sharcnet.ca) and Compute/Calcul Canada.

Dedication

This is dedicated to my family and friends.

Table of Contents

List of Tables

List of Figures

Chapter 1

Introduction

Accurate and individualized measurement and modeling of gait is useful in many applications, such as fall risk assessment [44], [60], biometrics [17], [13], [12], health characterization [1], localization [30, 34, 22, 11], and control of assistive devices such as prostheses [42], [19], exoskeletons [31], and functional electrical stimulation devices [59, 55, 58].

An important application of accurate gait modeling and assessment is fall risk assessment. Falls are the primary cause of injury among older Canadians and account for 40% of admissions to nursing homes, 62% of injury-related hospitalizations, and almost 90% of hip fractures [4]. They are the leading cause of injury-related death and hospitalization in old age, with over one third of older adults falling once or more each year [15]. Further, as the population continues to age [25], these rates will continue to increase [51].

Improved gait monitoring could be used to alert individuals when falls are likely to occur and propose solutions to reduce this likelihood. For example, there is a correlation between gait asymmetry and a person's likelihood of falling [24, 40, 61]. The ability to identify fall risk before a fall event has the potential to improve our ability to prevent falls, improving the health and quality of life of the elderly, and preventing costly and painful fall injuries. Furthermore, the ability to continuously monitor the evolution of gait through non-intrusive monitoring has the potential to facilitate early detection and assessment of many other health conditions, including musculo-skeletal disorders and injuries, stroke, Parkinson's disease and others.

1.1 Thesis Contributions

The main contribution of this thesis is the implementation of a complete framework and an accurate online gait event identification algorithm which is not dependent on a specific gait signal type; the framework was validated on both a healthy and pathological gait dataset.

Online Gait Model Learning

Gait characteristics differ for each individual and may also differ between legs for individuals with asymmetric gait. Furthermore, within a single individual, gait characteristics may change over time due to aging, disease or injury onset and progression, or as a result of treatment or interventions. To obtain an accurate, individualized model of gait, we propose to learn an individualized model of gait online during observation, using incremental updates to the model parameters based on the error between the model-predicted and measured signal. The algorithm can be applied to any input signal, which allows for more convenient measurement in daily living environments.

Complete Algorithm Framework

We implement a complete algorithm framework to identify gait events from any gait data. Since it is common for older walkers to take breaks and pause briefly when their gait data is collected in real-time, we first propose an activity recognition implementation to detect when someone is in fact walking. Once gait has been detected, the gait model is learned based on the input signal. We present three methods for selecting the gait model learning rates based on the application. We then propose a set of convergence criteria to ensure the gait model has been learned before proceeding to the identification of gait events.

Two methods of gait event identification were implemented: analytical event identification and initial event identification. If we know the properties of the gait events of interest, we can use the analytical event identification method. Alternatively, manual identification of a single gait event can be used to identify all future events using the initial event identification method.

Validation on Two Datasets

Our approach is implemented and tested on two datasets: one measuring mediolateral angular velocity of the ankles from a healthy and relatively young group of adults and

the other measuring sagittal linear acceleration of the ankles from a much older group of retirement home residents who each have a variety of medical conditions. For both datasets, the proposed approach has an average absolute error close to 0.03 gait cycles.

1.2 Thesis Outline

The remainder of the thesis is organized as follows:

Chapter 2 provides background information and an overview of gait event identification related work, including the signals collected and algorithms applied. We classify gait event identification algorithms along three axes: heuristic versus data-driven, specific versus arbitrary measurement signal type, and online versus offline.

Chapter 3 describes the proposed algorithm. Specifically, we first identify whether a signal is in fact gait, as it is common for older walkers to take a break and/or pause briefly during gait data collection. Once gait has been detected, we begin learning the gait model based on the input signal. We then ensure the gait model has been learned before identifying gait events. The gait model, activity recognition, convergence criteria, and event identification are each described. We detail two methods of event identification: analytical event identification and initial event identification.

Chapter 4 describes the implementation of the proposed algorithm on a young adult dataset with simulated pathologies, measuring ankle medio lateral angular velocity. The ground truth identification of foot impact and foot takeoff are measured using force sensors. The dataset as well as the parameter selection are described. The accuracy of the initial event identification method is validated. We also illustrate the utility of the algorithm by segmenting and plotting gait cycles with respect to time and phase.

Chapter 5 describes the implementation of the proposed algorithm on an older adult dataset, measuring ankle sagittal linear acceleration. The ground truth identification of initial swing events are identified with the help of a program which allows users to verify each event manually. The dataset, data processing, and parameter initialization are described. We also evaluate the selection of learning rates in more detail, analyzing a set of default, group optimized, and individually optimized learning rates. We propose a variety of performance metrics and validate the accuracy of both event identification methods and each set of learning rates against these metrics. We also compare our implementation to other peak detection methods.

Finally, Chapter 6 discusses the strengths and limitations of the proposed approach. In particular, we discuss the choice of event identification method, the choice of optimization

weights, a comparison to related work, limitations when applying the method to an arbitrary gait signal and on gait model learning, as well as real-time processing requirements for various applications. We then summarize the main conclusions and provide directions for future work, including an alternate evaluation approach, online parameter adaptation, using a multivariate gait model, gait recognition, using prior gait knowledge, and providing user diagnostics.

Chapter 2

Related Work

Gait event identification is implemented using a variety of sensors and algorithms. We first provide some background information and then provide a brief overview of gait event identification related work, including the signals collected and algorithms applied.

2.1 Background

A brief background on gait, periodic signals, and clinical gait analysis is provided in this section.

2.1.1 Gait

Human walking is defined as "a method of locomotion involving the use of the two legs, alternately, to provide both support and propulsion, with at least one foot being in contact with the ground at all times" [37]; while gait is defined as "the manner or style of walking" [37]. The gait cycle is defined as "the time interval between two successive occurrences of one of the repetitive events of walking" [37]. We call these repetitive events of walking *gait events*; they re-occur at the same location each gait cycle. Major gait events are shown in Figure 2.1.

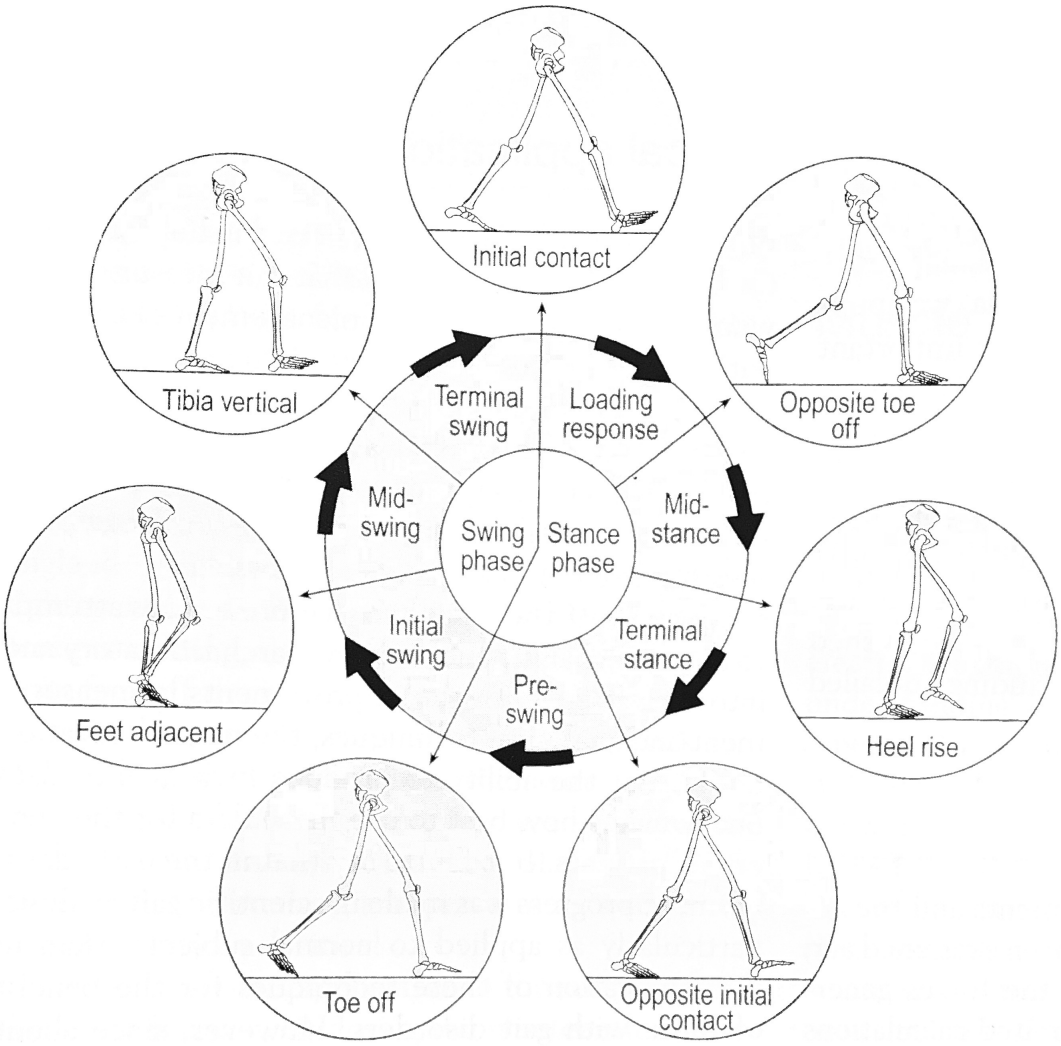

Figure 2.1: Typical Gait Cycle [37]

2.1.2 Periodic Signals

Any periodic signal, f, can be represented by a Fourier series (a sum of sinusoids of different amplitudes and frequencies):

$$f(\phi) = \sum_{m=0}^{\infty} (\alpha_m \cos(m\phi) + \beta_m \sin(m\phi)) \tag{2.1}$$

From this equation, we see that f will evaluate to the same value when an odd multiple of 2π is added to ϕ (*i.e.*, $f(\phi) = f(\phi + 2\pi n), \forall n \in \mathbb{Z}$). Therefore, we can think of ϕ as increasing cyclically from 0 to 2π, wrapping back around to 0 each time 2π is reached. In this way, we are able to associate each value of ϕ with a particular value of f; we call ϕ the *phase* of the signal.

Since gait is periodic, we are similarly able to associate each location of the gait cycle with a particular gait event. We can therefore think of each location of the gait cycle as having a corresponding phase, $\phi \in [0, 2\pi)$; we refer to this as the gait event phase. Each angle associated with a point on the circle in Figure 2.1 represents a gait event phase and is associated with a gait event corresponding to an instance of the gait cycle.

2.1.3 Gait Assessment in Clinical Settings

Most gait analysis in clinical settings is based on visual observation which lacks sensitivity. Sometimes quantitative measures such as Timed Up and Go [50], [65], [49] and timed gait trials [54], [20] are used, but these only indirectly measure the quality of motion. More advanced quantitative gait analysis techniques, such as the GAITRite [46] and motion capture systems [8], [26], can be used for gait event identification and subsequently the calculation of gait parameters, but are typically expensive and time-consuming to set up, and constrain the area where data can be collected.

2.2 Sensors

A large variety of signals have been used to identify gait events including linear acceleration [3], [58], angular velocity [68], [57], in-shoe force sensors [59], and a combination thereof [55]. Electromyography [35], goniometer [48], satellite positioning system [64], platform pressure [46], video-based, [63], and motion capture [8], [26] data have also been used.

However, video-based (*e.g.,* Kinect), platform pressure (*e.g.,* GAITRite, StepScan, Zeno walkway, TekScan Strideway), and motion capture (*e.g.,* VICON, Xsens, OptiTrack, Qualisys) systems are limited in terms of capture area and require equipment installation in the environment. Pressure based systems are typically considered the lab standard for identifying major stance events (*e.g.*, initial contact, opposite toe off, heel rise, opposite initial contact, toe off) [68], [28], [2], [71], [43], [66], [21]. Motion capture systems are also commonly used in lab settings for detecting gait events [62], [36].

2.3 Algorithms

There are three important distinctions used to classify gait event identification algorithms: heuristic versus data-driven, specific versus arbitrary measurement signal type, and online versus offline. Although offline event identification algorithms are useful for many applications, real-time health monitoring applications require online event identification. In these applications, the preferred gait event identification algorithm is data-driven, can be applied to any gait measurement signal, and can be implemented in real-time. It is desirable to use an online algorithm which generates a richer, more representative individualized model that generalizes to a large variety of input data.

2.3.1 Heuristic

The majority of gait event identification algorithms are based on heuristics, many of which are threshold-based [39], [73], [72], [38], [56], [67], [30], [11], [10], making them sensitive to threshold parameters and causing poor generalization to new data (*e.g.*, different gait type, ground surface, sensor placement, footwear, etc.).

For example, Aminian et al. [3] propose an offline heuristic event identification algorithm where thigh linear acceleration in the sagittal plane is collected. They identify global maxima within the smoothed acceleration signals and approximate the average gait cycle length by taking the average difference between these maxima. Heelstrike and toe-off events are identified as the global minima in the intervals 15% to 30% of the estimated gait cycle length following and before each maximum, respectively. The mean left and right stance over 16 consecutive gait cycles for 30 healthy participants had a 95% confidence interval within 0.02 seconds of the corresponding force pressure ground truth measurements.

Jasiewicz et al. [28] propose an online heuristic event identification algorithm where linear acceleration signals from the feet and angular velocity signals from the feet and

shanks were collected. Three different implementations were analyzed in which minima, maxima, or zero-crossings were identified as events within windows defined relative to the maximum dorsi and plantar flexion times (estimated from the gyroscope data). Foot contact was identified with an average error of 10-15 milliseconds for 26 healthy volunteers, for all methods; whereas it was identified with an average error of 15-55 milliseconds for 9 volunteers who had abnormal footfall.

González et al. [18] propose an online heuristic event identification algorithm in which vertical and sagittal accelerations are measured from the lower trunk and a set of heuristic rules were extracted from the training dataset to identify gait events. There was an average error of 13 milliseconds when identifying foot contact events on the test dataset collected from 6 individuals instructed to walk 12 times along a 10 meter path.

Hanlon and Anderson [21] propose an online heuristic event identification algorithm where linear acceleration and foot pressure data were collected. The footswitch force threshold algorithm had a foot contact mean absolute error of 2.4 milliseconds whereas the accelerometer algorithm had a foot contact mean absolute error of 9.5 milliseconds. Their accelerometer algorithm requires two accelerometers (one at the ankle and one at the knee) which have sampling rates of 1000 Hz. Training and test data were collected in the same controlled environment, with the same ground surface and accelerometer attachment sites, from twelve healthy participants. 41 accelerometer event identification algorithms were developed based on the training dataset and the above results were the best of all these algorithms when applied to the test dataset.

Finally, Zhu et al. [74] propose an online heuristic event identification algorithm in which frontal angular velocity signals are thresholded to detect heel impact and toe takeoff events. A stride length error of approximately 3% was reported; however, this method was only tested on five healthy individuals.

2.3.2 Data-Driven

A number of machine learning techniques have been proposed for gait event identification, including neural networks [47], [58], hidden Markov models [41], fuzzy logic [48], [59], and combinations thereof [35]. While these implementations are data-driven, they use offline training and do not generalize well to data that is different from the training set.

López-Nava and Muñoz-Meléndez [27] propose an online data-driven event identification algorithm in which thresholds on the acceleration signal are used to extract peaks in sagittal and vertical directions. A trained Bayesian classifier is then used to determine

whether a peak corresponds to a stride. An accuracy of 98% was reported for stride detection; however, the thresholds and Bayesian classifiers must be set differently for different age users.

Aung et al. [5] propose an offline data-driven event identification algorithm in which accelerometer data is collected from the foot, ankle, shank, and waist. The continuous wavelet transform is applied to each tri-axial signal, manifold embedding is then used to select a reduced number of features at each timestamp from those extracted at each wavelet scale and from each axis, and finally, a Gaussian mixture model is used to classify each time-stamp as a heel strike, a toe off, or no event. Using a temporal tolerance of 0.05 seconds and leave-one-out cross validation across eight healthy participants, they found a combined F1 score ranging from 76% to 86%, depending on the accelerometer location.

Miller [47] proposes an online data-driven event identification algorithm in which a neural network with one hidden layer is used to classify foot-contact and foot-off events using motion capture data of sagittal plane heel and toe marker coordinates. When comparing their event identification to force plate data, there was an average error of 8.8 milliseconds and 3.3 milliseconds for barefoot and shoe/braced pathologic subjects, respectively.

Alternatively, Mannini et al. [41] propose an online data-driven event identification algorithm in which a hidden Markov model consisting of stance and swing states was used to identify foot strike and toe off events using linear acceleration and angular velocity data from each ankle in real-time. When compared to the GAITRite ground truth data, they found average errors of 20 milliseconds and 16 milliseconds for foot strike and toe off events across their dataset of 10 older adults, 10 hemiparetic patients, and 10 Huntington's disease patients.

2.3.3 Specific versus Arbitrary Measurement Signal Type

Almost all gait event identification algorithms depend on the use of a specific measurement signal. Machine learning techniques allow new models to be created that are specific to a chosen measurement signal, but require a large dataset and corresponding period of offline training, each time the use of a new measurement signal is desired. Ideally, a gait event identification algorithm would not be dependent on a specific measurement signal type.

The application of the continuous wavelet transform has been shown to identify heel strike and toe off events from accelerometers attached at varying orientations and locations on the body, by identifying wavelet features (frequency characteristics associated with various scales of granularity) associated with each event [5], [33]. However, neither Aung

et al. [5] nor Khandelwal and Wickstrom [33] apply this to pathological gait data, non-accelerometer gait data, or the identification of other gait events. Aung et al. [5] find a 10% difference in F1 score, based on the chosen accelerometer location.

In addition to algorithms specifically designed for gait analysis, generic time series data processing algorithms can be applied. Yang et al. [70] survey a number of offline heuristic peak detection methods, generally consisting of smoothing, baseline correction, and peak finding components. Billauer [7] proposes an online heuristic peak detection algorithm. Local maxima and minima are searched for alternately, such that the identified maxima/minima is some threshold greater than or less than the previously identified minima/maxima. Because these are generic peak detection algorithms, unlike all of the above event identification algorithms, they do not require a specific signal type. However, they can only be used to identify peaks and not other signal characteristics.

2.3.4 Canonical Dynamical System

Righetti et al. [53] propose an adaptive oscillator which can learn the frequency of any periodic or pseudo-periodic signal. Petrič et al. [52] extend this work by using a Fourier series representation to identify the fundamental frequency, providing a measure of the energy content for multiple frequency components. They call this implementation the canonical dynamical system (CDS).

Recently, Joukov et al. [32] proposed an approach for gait pose estimation from wearable inertial sensors, using a rhythmic extended Kalman filter (EKF). Gait patterns are modeled using a Fourier time-series representation to estimate measured angular velocity terms. For this approach, the CDS model of gait is learned during online observation, which is then used to segment the motion data into strides based on the phase, with a segmentation accuracy of 97%.

2.4 Summary

This chapter provided background information and an overview of gait event identification related work, including signals which are collected and algorithms which are applied. We classify gait event identification algorithms along three axes: heuristic versus data-driven, specific versus arbitrary measurement signal type, and online versus offline. The most desirable classification is data-driven, can be applied to any measurement signal type, and can be run in real-time; the CDS satisfies all three of these classifications.

In this thesis, we propose to use the CDS to model gait as a periodic signal. The estimated phase within each stride can then be used to identify and align gait events that occur from stride to stride, from trial to trial, and from individual to individual.

Chapter 3

Methods

This thesis proposes a method to learn a model of the gait cycle online from any measured gait signal. The gait data is modeled as a periodic signal with a continuous phase variable, allowing data to be automatically labeled with a phase value corresponding to a particular event that re-occurs each gait cycle. This model can be used to directly calculate gait parameters as well as their variability over multiple gait cycles.

When gait data is collected in real-time from an older population, it is common for walkers to take a break and/or pause briefly. Therefore, we must first detect when someone is in fact walking. Once gait has been detected, we begin learning the gait model based on the input signal. We then ensure the gait model has been learned before identifying gait events. These four steps are illustrated in Figure 3.1. This section describes the gait model, activity recognition, convergence criteria, and event identification[1].

3.1 Gait Model

We model gait using the CDS Fourier series representation introduced by Petriĉ et al. [52], described by:

$$\hat{y}_t = \sum_{m=0}^{M} \left(\alpha_{m,t} \cos\left(m\phi_t\right) + \beta_{m,t} \sin\left(m\phi_t\right)\right) \tag{3.1}$$

[1] An early version of this chapter has been submitted in [69]

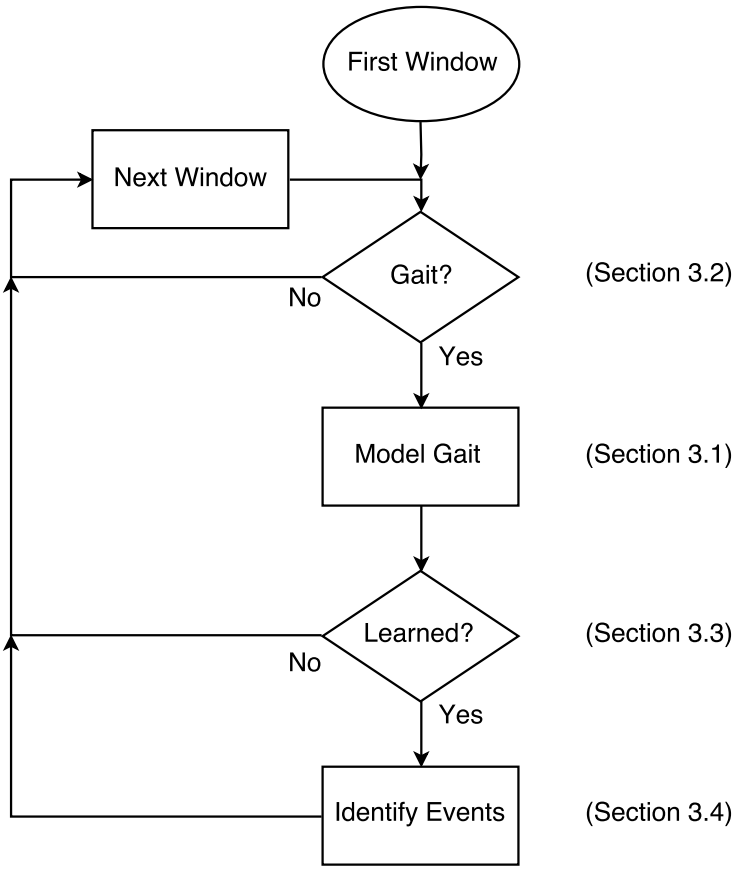

Figure 3.1: At each time step, the algorithm determines whether the input signal is gait, based on the previous window of data. If the signal is determined to be gait, the algorithm will update the gait model. It will then verify that the gait model is an accurate representation of the gait signal. Finally, if the model has been learned, the algorithm will identify gait events. Each component of the algorithm is described in Section 3: activity recognition in Section 3.2, the gait model in Section 3.1, the convergence criteria in Section 3.3, and event identification in Section 3.4

where $\hat{y}$ is the estimated signal, M is the number of harmonics in the estimated signal, α_m and β_m are the m^{th} frequency coefficients of the estimated signal, ϕ is the estimated phase, and subscript t denotes the corresponding variable value at time t. To learn the model, the system parameters are updated as follows:

$$\begin{aligned} e_t &= y_t - \hat{y}_t \\ \phi_{t+1} &= mod(\phi_t + T(\omega_t - \mu e_t \sin(\phi_t)), 2\pi) \\ \omega_{t+1} &= |\omega_t - T\mu e_t \sin(\phi_t)| \\ \alpha_{m,t+1} &= \alpha_{m,t} + T\eta e_t \cos(m\phi_t) \\ \beta_{m,t+1} &= \beta_{m,t} + T\eta e_t \sin(m\phi_t) \end{aligned} \tag{3.2}$$

where y is the actual signal, e is the error between the estimated and actual signal, ω is the estimated angular frequency[2], μ is the frequency learning rate, η is the coefficient learning rate, and T is the sampling period. We further constrain the phase to be monotonically increasing.

The variables above can be divided into a set of adaptable parameters which are updated with t as the incoming signal is learned (ϕ, ω, α, β) and a set of constant parameters which are predetermined (M, μ, η).

To initialize a model, we start with initial values for the adaptable and constant parameters. The adaptable parameters will then be updated based on the incoming data to create a model that more closely describes the data. The error between the estimated and the measured signals will be used at each time step to update the adaptable parameters. Figure 3.2 illustrates the learning process.

3.2 Activity Recognition

Participants who experience walking difficulties may need to pause or stop between series of steps. Activity recognition is used to ensure that gait parameter learning only occurs during active gait. When the signal is determined to be active (meaning walking is occurring), the gait modeling algorithm is continuously run. On the other hand, when the signal is determined to be inactive, the gait model is no longer adapted, rather the previously learned gait model is retained (*i.e.* cadence as well as magnitude coefficients associated with each frequency component).

[2]The angular frequency is equal to the cadence since gait events repeat each gait cycle (where angular frequency is the frequency multiplied by 2π).

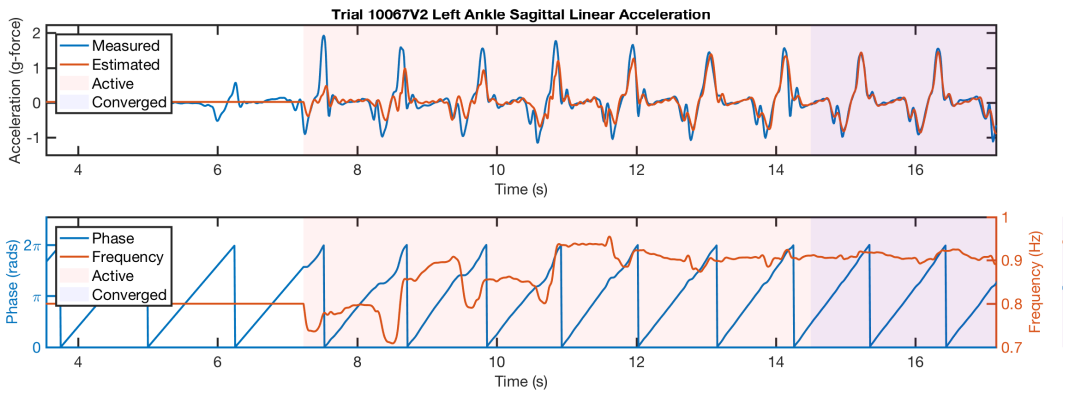

Figure 3.2: Learning of a Gait Model. The top panel shows the measured older adult left ankle sagittal linear acceleration in blue and the corresponding estimate (using default learning rates) in orange; after approximately six gait cycles, the estimated signal converges to the actual signal. The red background denotes times at which the measured signal was deemed to be active (see Section 3.2) and the blue background denotes times at which the estimated signal met the convergence criteria (see Section 3.3). The bottom panel shows the estimated phase in blue (left vertical axis) and the estimated frequency in orange (right vertical axis).

We assume that data collection starts from an inactive state. For the initial recognition of activity, the standard deviation across the previous window of input (from sample $t - wl+1$ to sample t, where wl is the window length), σ_t, must be greater than some threshold, T_a:

$$\sigma_t > T_a \longrightarrow Active$$

As the signal is read, the algorithm keeps track of the largest standard deviation of all sliding windows since the start of the signal, σ_{max}. Once an active state has been reached, the signal is deemed inactive if the standard deviation across the previous window is less than one third of the maximum standard deviation across all previous windows:

$$\sigma_t < \frac{1}{3}\sigma_{max} \longrightarrow Inactive$$

Similarly, to return to an active state, the standard deviation across the previous window must be greater than one half of the maximum standard deviation across all previous windows.

$$\sigma_t > \frac{1}{2}\sigma_{max} \longrightarrow Active$$

Each time an inactive state is reached, the model parameters ω, α, and β are set to the values they were N_a windows prior to the inactivity. This ensures that the model learns steady-state gait, as opposed to the transition from activity to inactivity.

3.3 Convergence Criteria

Before events can be identified based on the phase estimated by the gait modeling algorithm, the predicted signal should have converged to the actual signal. We evaluate this measure of convergence based on absolute differences between the estimated and actual signals over the previous window, only after the signal has been deemed active (see Section 3.2). We present two different implementations of convergence criteria: error based and ratio based.

3.3.1 Error

For the error convergence criteria, we assume convergence has been reached (the model has been learned) once the sum of the average absolute error over the previous window is below some threshold, T_{ce}.

3.3.2 Ratio

For the ratio convergence criteria, we assume convergence has been reached once the ratio of the average absolute input signal from the previous window over the average absolute estimated signal from the previous window is within some threshold, T_{cr}. Therefore, for a model to meet convergence criteria, it must already have been deemed active and the estimated and actual signals must have approximately the same amplitude over the previous window.

Note, this method was used after finding that using the error between the signal and the estimate to determine convergence was less robust to variations in noise and signal-to-noise ratios.

3.4 Event Identification

Once the estimate has converged to the actual signal (the gait model has been learned), we wish to identify the gait events. We use two methods to accomplish this goal: analytical event identification and initial event identification.

3.4.1 Analytical Event Identification

Since we learn a gait model that has an analytical representation, if we know the properties of the gait events of interest, we can use the model to compute the corresponding phase. For example, to identify the peak event in each gait cycle, we can solve for the phase which generates the maximum value and assign this as the peak phase value.

The estimated peak phase is updated each time the phase which is π away from the current peak phase, is passed. This is to avoid events being identified more than once. For example, if the peak phase were to be shifted slightly forward and updated right after an event had been identified, it could be identified twice by the algorithm.

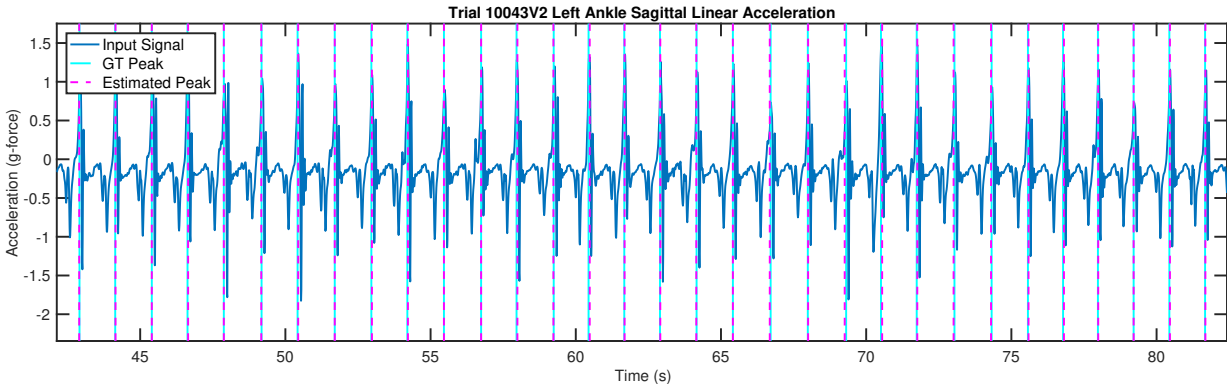

Figure 3.3: Analytical CDS and Ground Truth Event Identification. The blue line shows a left ankle sagittal linear acceleration signal taken from the older adult 6MW dataset. The vertical cyan and dotted pink lines show the peak events, as identified by the analytical event identification algorithm (using optimized learning rates) and the ground truth manual labelling, respectively. The estimated peak events closely track the ground truth events.

Analytical event identification is shown in Figure 3.3, for peak events. We see the estimated events align closely with the ground truth events for each gait cycle.

3.4.2 Initial Event Identification

An alternate approach is needed if we do not know the analytical characteristics of the gait event(s) of interest. Once gait events are identified relative to the estimated gait phase, we can automatically identify any future events since we assume they occur at the same phase, as is common in gait analysis [45]. The phase corresponding to an event is identified in the first gait cycle that meets the convergence criteria (see Section 3.3) and then all events in subsequent strides are identified when that same phase value is reached again.

Each time inactivity occurs or convergence criteria cease to be met, the estimated peak phase is updated only upon reaching the first GT event in which convergence criteria are met. We identify this first event in two ways: manually and using heuristics.

Manual

In this approach, we provide a manual identification of a gait event for a single gait cycle. Initial manual event identification is shown in Figure 3.4, for peak events. We see the estimated events align closely with the ground truth events for each gait cycle.

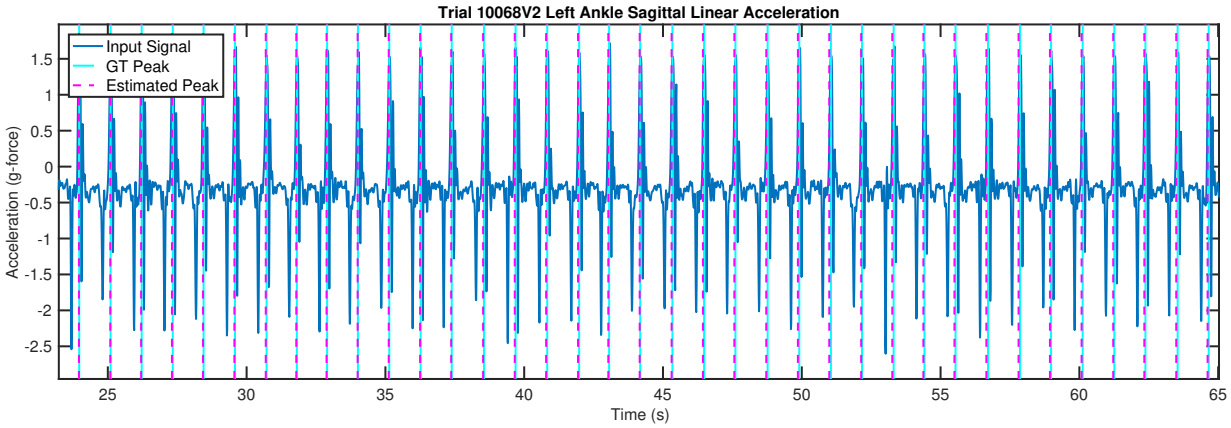

Figure 3.4: Initial CDS and Ground Truth Event Identification. The blue line shows a left ankle sagittal linear acceleration signal taken from the older adult 6MW dataset. The vertical cyan and dotted pink lines show the peak events, as identified by the initial manual event identification algorithm (using optimized learning rates) and the ground truth manual labelling, respectively. The estimated peak events closely track the ground truth events.

Heuristic

To identify an event relative to the gait phase determined by the model, we developed heuristics based on ankle frontal angular velocity signals motivated by [73], to identify the gait events as follows:

- Heel impact: The phase of the first local minimum following the maximum value (cycle values are re-ordered to start at the index of the maximum value and wrap around to the index prior);
- Toe takeoff: 1.25π after the heel impact event.

Since the heel impact event is the easiest to identify heuristically and because we observed that toe takeoff often occurs approximately 1.25π after heel impact, we identify the toe takeoff (TT) event *relative* to the heel impact (HI) event.

This method of event identification is shown in Figure 3.5 for heel impact and toe takeoff events. The estimated events are similar to those obtained from the ground truth data.

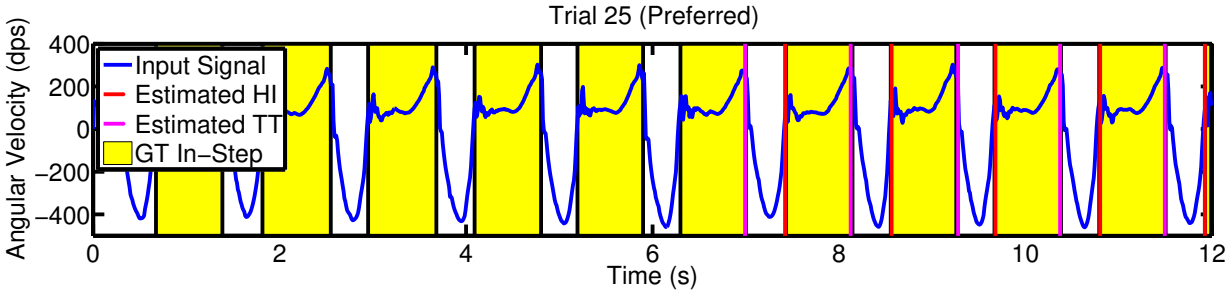

Figure 3.5: Initial Heuristic CDS and Ground Truth Event Identification. The blue line shows the left ankle frontal angular velocity signal from the young adult dataset. The vertical red and pink lines show the HI and TT events, respectively, as identified by the heuristic event identification. The starts and ends of sections highlighted in yellow show the locations of HI and TT events identified from GT data, respectively. As desired, vertical red lines coincide with the starts of highlighted sections and pink lines coincide with the ends of highlighted sections.

However, because inertial measurement unit (IMU) data is very sensitive to orientation changes that cannot be perfectly controlled and heuristic methods are sensitive to the signal form, this method does not work correctly for all data.

3.5 Summary

In this chapter we proposed an online algorithm for gait modeling and event detection. We first detect when someone is in fact walking as it is common for gait data from older populations to contain rests and pauses. Once gait has been detected, the gait data is modeled as a periodic signal, which is incrementally updated based on the error between the model-predicted and measured signal. Since the model has a continuous phase variable, data is automatically labeled with a phase value corresponding to a particular event that re-occurs each gait cycle. Once the model has been learned, we identify gait events using analytical or initial event identification. Analytical event identification directly computes the gait event phase from the gait model, when we know the properties of the gait event. Initial event identification uses an initial labelling of a specified gait event to automatically identify all future events, since we assume they occur at the same phase.

Chapter 4

Young Adult Dataset

This chapter describes the implementation of the proposed algorithm on a young adult dataset[1] with simulated pathologies, measuring ankle medio lateral angular velocity. We first describe the experimental protocol and then describe the results when using the proposed approach on this dataset. Since this dataset contains only steady-state gait, activity recognition (see Section 3.2) was not implemented.

4.1 Experimental Protocol

This section describes the experimental protocol, including the data collection, parameter initialization and algorithm settings, as well as the ground truth processing.

4.1.1 Data Collection

Data from 16 healthy participants was collected at the Neuroscience, Mobility and Balance lab at the University of Waterloo (67% male, age = 25±4 years, height = 171±5 cm, weight = 66 ± 10 kg). Subjects were asked to do a variety of gait types, including walking at their preferred pace, walking using a walker, walking using a cane, walking slowly, walking with a simulated single limb impairment (asymmetric), walking in a large circle, and walking at varying speeds (slow-fast-slow). Slow, preferred, and fast speeds were self-selected. The trials were either 12.2 or 19.9 meters in length, with the exception of the turn trials, which were each approximately 41.7 meters.

[1] An early version of this chapter appeared in [68]

Both linear acceleration and angular velocity (along sagittal, frontal, and vertical axes) were collected from Shimmer[2] IMUs attached to individuals' right ankle, left ankle, right hip, and sternum. Accelerometer and gyroscope data was collected at 102.4 Hertz with sensitivities of ±(2-8) G-force and ±500 degrees per second (dps) respectively. For ground truth measurements, Bortec[3] footswitch cells were placed at the toe and heel of each subject's foot, either under the insoles or directly under the shoes.

A total of 285 trials were used. The study was approved by the University of Waterloo Research Ethics Board and consent was obtained from all participants, following a pilot data collection.

While the proposed method can be applied to any continuously measured signal, here we use the left-ankle frontal (Y-axis) gyroscope signal. We chose this as input since gyroscope data is less noisy than accelerometer data and the angular velocity along the frontal axis intuitively carries the most information for lower limb motion. We have discarded all other information because only one signal is necessary to determine the phase of the gait cycle; once this phase is learned, it can be applied to all measured signals.

4.1.2 Parameter Initialization and Algorithm Settings

The parameter initialization values were chosen empirically and are as follows: $\omega = 2\pi(\frac{3}{4})$ rads/s $= \frac{3}{4}$ Hz; $\phi = 0$; $\alpha_m = 10, \forall m$; $\beta_m = 5, \forall m$; $M = 6$; $\mu = 0.01$; and $\eta = 1$.

For the adaptable parameters, these are only initial settings adapted during online observation; however, the closer the initial guesses are to their true values, the more quickly the algorithm is able to learn the corresponding model. While moderate intensity walking is approximately 100 steps/min (50 gait cycles/min) [45], we plan to apply this algorithm to a large variety of gaits, including much slower gaits. We also want the fundamental frequency to coincide with the subject's cadence and therefore need to be careful that our initial frequency is not closer to a multiple of the fundamental frequency than to the fundamental frequency. Hence, we have chosen our frequency, ω, to be 45 cycles/min $= \frac{3}{4}$ Hz. Figure 4.1 shows the learning of a gait model using parameter initializations as described above.

Set parameter values are shown in Table 4.1. The window length, wl, was chosen to include at least one complete gait cycle so that the entire gait cycle is evaluated when determining whether the model has been learned. Increasing wl further results in increased

[2]Shimmer Research, www.shimmer-research.com
[3]Bortec Biomedical Ltd., www.bortec.ca

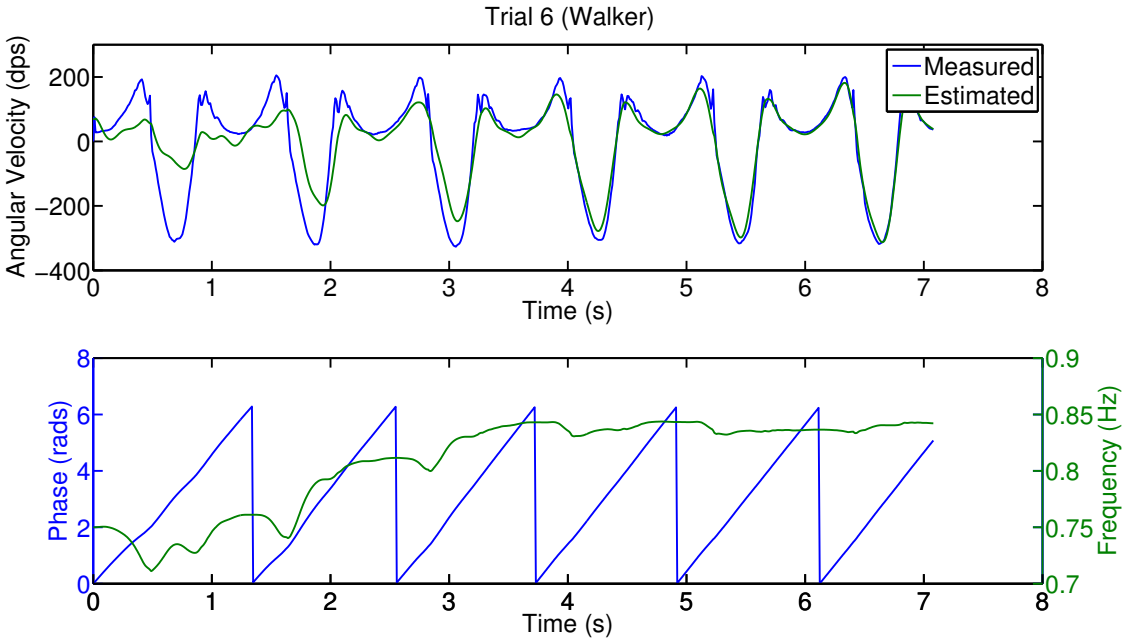

Figure 4.1: Learning of a Gait Model. The top panel shows the measured left ankle frontal angular velocity from the young adult dataset in blue and the corresponding estimate in green; after five cycles, the two signals appear almost identical. The bottom panel shows the estimated phase in blue (left vertical axis) and the estimated frequency in green (right vertical axis).

Table 4.1: Set Parameter Values

Parameter	**Value**
M	6
μ	0.01
η	1
wl	150 samples = 1.5 seconds
T_{ce}	30 deg/s

delay in identifying when the model has been learned; hence, increasing the convergence time. The remaining parameters were chosen empirically.

We use the error convergence criteria for this implementation and evaluate both manual and heuristic initial event identification methods.

4.1.3 Ground Truth Processing

Each footswitch cell is the size of a large coin. Two footswitches are used per foot (either under the insole or under the shoe), one at the toe (to capture the toe takeoff event) and one at the heel (to capture the heel impact event). Wires from each of the two footswitches measuring data from each foot are combined, meaning only one signal is captured per foot.

The (combined) footswitch signal is generally close to 0 millivolts (mV) when there is no pressure on either of the footswitches and 2600 mV when there is pressure on one or both of the footswitches. Because footswitches are only placed at the heel and the toe, the signal sometimes drops during the stance phase if there is only pressure on the middle of the foot, in between the heel and the toe footswitch cells.

To clean the footswitch data so that it can be consistently read, we use signals from both feet to process the data, where our goal is to remove drops during the stance phase. Since we are using gait data, we assume that at least one signal should be at a maximum (conceptually this means that there is pressure on at least one of the subject's feet). If both signals were at a minimum, this should indicate that neither foot was on the ground.

A minimum threshold of 500 mV and a maximum threshold of 2000 mV are used to account for noise. At each point in time, if there is no pressure detected on either foot, we force the signal of the foot that most recently had pressure to its previous value (that was greater than or equal to the maximum threshold).

A heel impact event is identified when a signal's previous 20 values were all below the minimum threshold and its current value is above the minimum threshold. Similarly, a toe takeoff event is identified when a signal's previous 40 values were all above the maximum threshold and its current value is below the maximum threshold. In Figure 3.5, these ground truth events are shown as the start of the highlighted section (heel impact) and the end of a highlighted section (toe takeoff). 18 trials in which footswitch data contained too much noise to reliably identify events were discarded (the processing defined above did not yield alternating heel impact and toe takeoff events).

4.2 Results

The initial event identification method is compared to GT data by a validation routine that measures both the accuracy of the algorithm and the amount of time it takes to meet the error convergence criteria (see Section 3.3.1). The accuracy measurement focuses on the recognition of heel impact and toe takeoff events of the gait cycle. We also evaluate the usefulness of the algorithm by segmenting and plotting gait cycles with respect to time and phase.

4.2.1 Performance Analysis

Three values of particular interest are the percentage of trials that meet the convergence criteria, the time these trials take to meet the criteria, and the error in estimated event times for these trials.

The impact event time error is computed by taking the absolute difference between each impact event identified by the CDS method and the corresponding impact event from the ground truth data. This means that if there is an error in the frequency estimation, the error could be larger than one cycle. For this reason, if the error is greater than one cycle, we set that error to the cycle length (taken to be the average length between impact events, as determined by the ground truth data). The takeoff event time errors are similarly computed; the overall event time error is taken as the average of the impact and takeoff event time error. To ensure that events identified by the CDS and the footswitches can be compared, if the CDS and ground truth event estimates finish with different event types, we remove the last event.

The results are shown in Table 4.2; 93% ($\frac{264}{285}$) of the trials met these criteria. The mean ($\pm$ standard deviation) is shown for each performance measure. The error criteria for

Table 4.2: Performance Measures

	Seconds	**Cycles**
Initial Convergence Time	6.74 (±3.25)	5.46 (±2.38)
Event Time Error		
Heuristic	0.11 (±0.15)	0.08 (±0.11)
Manual	0.05 (±0.12)	0.04 (±0.08)

convergence are met in about 5 strides. Initial manual event identification performs better than initial heuristic event identification, as expected. The heuristic approach results illustrate the achievable performance of the initial event identification if GT footswitch data is not available. Alternatively, the analytical event identification method can be used if the event signal characteristics necessary to develop heuristic event identification are known (see Section 6.1.1).

Table 4.3 shows the percentage of trials that met convergence criteria for each gait type, and of those, the associated initial convergence time and event time error when using manual event identification. Performance is excellent across a variety of gait types, including asymmetric and assisted gait. Note that a greater percentage (100%) of turn trials met convergence criteria than any other gait type. This is because these trials consisted of participants walking in a large circle which was more than double the length of all other gait types.

The varying speed trials contain most of the trials for which the algorithm did not meet convergence criteria; this is likely because the gait frequency continues to change and the algorithm does not always reach the convergence criteria before another change in speed occurs. We also see that varying speed trials have the greatest event time error; this is likely due to error that occurs as the algorithm learns a changed frequency (after already having met convergence criteria for a previously learned gait speed). Unlike the other gait types, the gait models for the varying speed trials are almost always in a learning state.

4.2.2 Segmentation

A segmentation algorithm was implemented that separates the data into segments, once the error criteria for convergence have been reached. Each segment is taken to be from one heel impact event to immediately before the next heel impact event. Data taken from one collection including all gait types except for varying speed is segmented and shown in

Table 4.3: Initial Manual Event Identification Performance with Gait Type. The first column indicates the gait type of the evaluated trials; the second column shows the percentage of trials that converged; the last two columns show the initial convergence time and the event time error, respectively, in cycles.

Gait Type	**Trials Converged**	**Initial Convergence Time**	**Error**
All	93% ($\frac{264}{285}$)	5.46 ($\pm$2.38)	0.04 ($\pm$0.08)
Preferred	90% ($\frac{60}{67}$)	6.35 ($\pm$1.63)	0.01 ($\pm$0.01)
Walker	99% ($\frac{66}{67}$)	5.39 ($\pm$1.81)	0.02 ($\pm$0.01)
Asymmetric	92% ($\frac{36}{39}$)	5.38 ($\pm$3.20)	0.04 ($\pm$0.05)
Slow	90% ($\frac{36}{40}$)	5.06 ($\pm$3.62)	0.06 ($\pm$0.11)
Cane	94% ($\frac{31}{33}$)	4.08 ($\pm$1.51)	0.05 ($\pm$0.06)
Large Radius Turn	100% ($\frac{23}{23}$)	6.32 ($\pm$1.76)	0.03 ($\pm$0.05)
Varying Speed	75% ($\frac{12}{16}$)	4.71 ($\pm$1.59)	0.27 ($\pm$0.22)

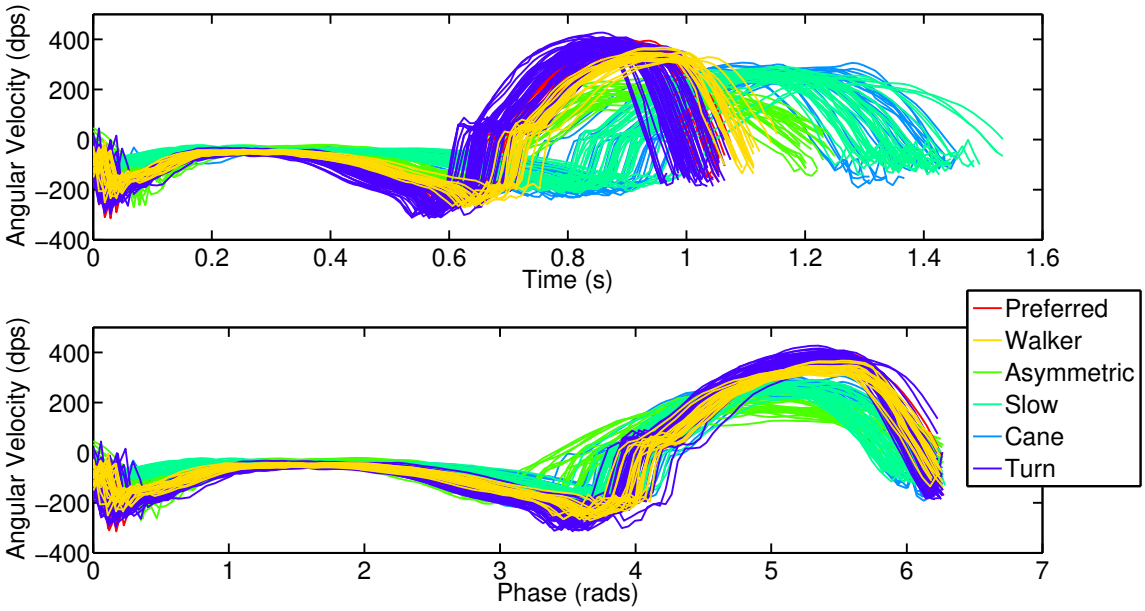

Figure 4.2: Data Segments Plotted with Time (top) and Gait Phase (bottom). Although both panels show the same data, it is clear that events occurring in each gait cycle correspond more closely when aligned with the estimated phase rather than time (both between strides and between trials).

Figure 4.2. The estimated phase variable allows the cycles, which are performed at various speeds, to be temporally aligned.

4.3 Summary

We implement the proposed approach on a young adult dataset with simulated pathologies, measuring ankle medio lateral angular velocity. The ground truth identification of foot impact and foot takeoff are measured using force sensors. The proposed approach converges within approximately five gait cycles and foot impact and foot takeoff events are extracted with an average error of 0.04 gait cycles, using the initial manual event identification method. We also evaluate the usefulness of the algorithm by segmenting and plotting gait cycles with respect to time and phase; it is clear that events occurring in each gait cycle correspond more closely when aligned with the estimated phase rather than with time.

Chapter 5

Older Adult Dataset

This chapter describes the implementation of the proposed algorithm on an older adult dataset[1], measuring sagittal linear acceleration of the ankles from a group of retirement home residents who each have a variety of medical conditions. We first describe the experimental protocol and then describe the results when using the proposed approach on this dataset.

5.1 Experimental Protocol

In this section we discuss the data collection and associated data processing, parameter initialization, algorithm settings, and learning rate selection, as well as ground truth processing.

5.1.1 Data Collection

Data was collected from participants (each having a variety of medical conditions) dwelling in four retirement communities in Ontario, Canada between 2010 and 2016. Of the trials collected from participants, there were 48 trials collected from participants who had fallen within the year prior to the collection, did not use an assistive device during the collection, and from whom Six-Minute-Walk (6MW) data was collected. Since there were significantly more trials available from participants who had not reported having fallen in the year

[1] An early version of this chapter has been submitted in [69]

prior to the collection, we took approximately the same number (50) of these trials which also satisfied the two latter criteria. Some of the trials were collected from the same participants longitudinally (approximately a year between each collection); in total our dataset consisted of 46 unique participants that had fallen in the year prior to the data collection, 47 unique participants who had not fallen in the year prior to the data collection, and 92 unique participants in total (61% female, age = 86 ± 5 years, height = 167 ± 9 cm, weight = 68 ± 12 kg). 31% of participants lived in condos (independent living), 68% lived in retirement homes (assisted living), and 1% lived in long-term care. Each participant had between 1 and 14 clinical diagnoses. On average, participants had 5 clinical diagnoses and had 7 medications on record.

Each participant was asked to do the 6MW test as part of their data collection. This test entailed the participant walking down a long hallway (varying in length depending on the retirement home and location of data collection), with an aide following closely behind for safety. They were told to walk as quickly but also as safely as possible and that they could stop for breaks as often as needed; if they made it to the other end of the hallway, they were instructed to turn around and continue going back and forth for a total of six minutes.

Linear acceleration (along sagittal, frontal, and vertical axes) were collected from Gulf Coast [2] accelerometers (X6-2, X6-2mini, X8m-3, or X16-2) attached to each individual's right ankle, left ankle, and right hip. Accelerometer data was collected at 40 or 50 Hertz with a sensitivity of $\pm$ 2, 8, or 16 G-force.

While the proposed method can be applied to any continuously measured periodic signal, here we use the left ankle sagittal linear acceleration signal. We chose this as input since the linear acceleration along the sagittal and vertical axes carry the most gait information and the signal from the sagittal axis was used in the manual ground truth event identification implementation. Additionally, the sagittal acceleration components contain both the impact at foot contact and the swing phase information.

The study was approved by the University of Waterloo Research Ethics Board and informed consent was obtained from all participants prior to the start of each data collection.

5.1.2 Data Processing

Before starting the data collection, all accelerometers were moved rapidly together, at the same time. A LabVIEW program was then used to time-align all accelerometer data using

[2]Gulf Coast Data Concepts, LLC, www.gcdataconcepts.com

the cross-correlation function. The data was also filtered using a low-pass 10 Hz 4th order Butterworth filter. The 6MW segment of the data collection was then manually extracted from the entire data collection activity log.

All data was resampled to 100 Hz using a spline approximation, to account for any sampling differences in accelerometer version and settings. At the same time, the mean value of each trial was subtracted from each datapoint to simplify the ground truth processing. To get the raw data into g-force units, it is divided by 1024.

5.1.3 Parameter Initialization and Algorithm Settings

The initial parameter values were chosen as follows: $\omega = 2\pi(\frac{4}{5})$ rads/s $= \frac{4}{5}$ Hz; $\phi = 0$; $\alpha_m = 0, \forall m$; $\beta_m = 0, \forall m$; and $M = 10$. The choice of the learning rates, μ and η will be discussed in Section 5.1.4.

For the adaptable parameters, these are only initial settings that are adapted during online observation; however, the closer the initial guesses are to their true values, the more quickly the algorithm is able to learn the corresponding model.

We initialized the α and β coefficients to zero since we do not have a strong prior on their values: they may be positive or negative and will vary significantly based on the gait measurement modality as well as the specific scenario (*e.g.,* the individual, shoes worn, ground surface, etc.).

On the other hand, we can incorporate prior knowledge of ω, based on typical human walking speed. While moderate intensity walking is approximately 100 steps/min (50 gait cycles/min) [45], our dataset contains a large variety of gaits, including much slower gaits. We want the fundamental frequency to coincide with the subject's cadence. Since the sizes of the basins of attraction which surround each frequency component are dependent on the energy content of the corresponding frequency component [9], the initial frequency should be close to the fundamental frequency. Hence, we have chosen our frequency, ω, to be 48 cycles/min $= \frac{4}{5}$ Hz.

We use the ratio convergence criteria for this implementation and evaluate both the analytical event identification method as well as the initial manual event identification method. The implementation of the analytical event identification method for peak gait events is described in detail in Appendix A.

Set parameter values are shown in Table 5.1. The majority of these parameters are used for activity recognition and convergence criteria. The window length, wl, was chosen to include at least one complete gait cycle so that the entire gait cycle is evaluated when

Table 5.1: Set Parameter Values

Parameter	Value
M	10
wl	150 samples = 1.5 seconds
T_a	$200 \approx 0.2$ g-force
N_a	2
T_{cr}	0.05

determining whether the model has been learned. Increasing wl further results in increased delay in recognizing activity and identifying when the model has been learned; hence, increasing the overall time required to learn the gait model and meet convergence criteria. N_a was chosen to be two windows so that the model parameters are set to values which represent steady-state gait and not the transition to inactivity, once inactivity is reached. T_a, T_{cr}, and M were chosen empirically.

5.1.4 Learning Rate Selection

The choice of learning rates determines the rate at which the gait model is learned. This rate is particularly important when people stop frequently when walking, as is common with those who have trouble walking. In this case, it is advantageous to learn the model very quickly. In our dataset, participants turn around and stop quite frequently so fast convergence is needed. Three learning rate implementations were analyzed: using a default set of learning rates, finding optimal learning rates for a group of training trials to apply to test trials, and individually finding optimal learning rates for each test trial. Each method is described below.

Default

Default learning rates were selected empirically, based on the implementation of the CDS algorithm with the healthy gait dataset, using ankle frontal angular velocity as the measurement signal. The default learning rates are $\mu = 0.01$ and $\eta = 1$.

Figure 3.2 shows the learning of a gait model using default learning rates and the parameter initializations described in Section 5.1.3. The main difference in parameter initialization for this older adult dataset, as opposed to the young adult dataset discussed

in Chapter 4, is that the number of harmonics in our model representation, M, has been increased to better model the larger frequency components due to increased noise in accelerometer signals, compared to gyroscope signals.

Individually Optimized

An optimization was run on each individual trial to determine the individually optimized learning rates. We desire learning rates which minimize differences between actual and estimated events while also reducing convergence times (both for previously unknown and previously known gait models). Further, we want the error between actual and estimated signals to be minimized.

The optimization finds the learning rate values which minimize the cost function, *i.e.*

$$\underset{\mu,\eta}{\operatorname{argmin}} J(\mu, \eta)$$

where the cost function associated with each trial is defined as:

$$J(\mu, \eta) = \begin{bmatrix} J_{PO} & J_{ER} & J_e & J_{CT} & J_{\alpha,\beta} & J_\omega \end{bmatrix} \mathbf{w}$$

with $\mathbf{w} = \begin{bmatrix} \mathrm{w}_{PO} & \mathrm{w}_{ER} & \mathrm{w}_e & \mathrm{w}_{CT} & \mathrm{w}_{\alpha,\beta} & \mathrm{w}_\omega \end{bmatrix}^{\mathrm{T}}$.

J_{PO} quantifies the phase offset error, *i.e.*

$$J_{PO} = \frac{1}{E} \sum_{i=1}^{E} PO_i^2$$

where PO is the phase offset, which is equal to the difference between the estimated phase at each GT event and the estimated peak phase (once ratio convergence criteria have initially been met), computed as a percentage of a gait cycle; and E is the number of GT events after the convergence criteria are initially met.

J_{ER} evaluates the ratio of the number of estimated events to the number of GT events; we call this the events ratio (ER), where

$$ER = \frac{\#Estimated\ Events}{\#GT\ Events}$$

Each event is counted only in sections in which GT events were recorded and in which estimated events were determined (the signal was deemed active and ratio convergence criteria were met). Ideally this ratio is equal to 1, therefore,

$$J_{ER} = (ER - 1)^2$$

J_e evaluates the mean squared error over the entire trial, normalized by the mean squared input, *i.e.*

$$J_e = \frac{\sum_{t=1}^{n} e_t^2}{\sum_{t=1}^{n} y_t^2}$$

J_{CT} evaluates the number of gait cycles it takes for the algorithm to meet ratio convergence criteria. Two measures are included: the initial convergence time (iCT) and the pre-learned convergence time (pCT). iCT is the number of gait cycles taken by the algorithm to meet ratio convergence criteria for the first time, relative to the beginning of that period of activity. pCT is the mean number of gait cycles taken by the algorithm to meet ratio convergence criteria, relative to the beginning of each corresponding period of activity, excluding the first time convergence criteria are met (*i.e.* after a model has been learned and there have been one or more periods of inactivity).

$$J_{CT} = iCT^2 + pCT^2$$

Note that pCT is only included in J_{CT} when the algorithm meets ratio convergence criteria more than once during a trial and J_{CT} is only included in the overall cost function when the algorithm meets ratio convergence criteria at least once.

The final cost functions, $J_{\alpha,\beta}$ and J_ω, are used to regularize the model parameters:

$$J_{\alpha,\beta} = \frac{\sum_{t=1}^{n} \sum_{m=0}^{M} (\alpha_{m,t}^2 + \beta_{m,t}^2)}{\sum_{t=1}^{n} y_t^2}$$

$$J_\omega = \frac{1}{n} \sum_{t=1}^{n} \omega_t^2$$

The weights were chosen empirically as follows: $w_{PO} = 0.5$, $w_{ER} = 0.1$, $w_e = 0.4$, $w_{CT} = 10^{-6}$, $w_{\alpha,\beta} = 10^{-3}$, and $w_{\omega} = 10^{-5}$. The optimizations were run in MATLAB using the local solver *fmincon* with multiple start points using *GlobalSearch* to sample multiple basins of attraction. The initial starting points were taken to be the default values, $\mu = 0.01$ and $\eta = 1$.

Group Optimized

The group optimized learning rates were determined using the same cost function as for the individually optimized learning rates. However, the group optimized parameters were determined based on five randomly selected trials from participants who had fallen in the year prior to the data collection and five randomly selected trials from participants who had not fallen in the year prior to the data collection. These trials made up the training set; the optimization finds the learning rate values which minimize the mean of the cost function across all training trials. The optimized training learning rates were then used on the remaining trials (the test set).

5.1.5 Ground Truth Processing

For ground truth measurements, a LabVIEW program was developed in which each peak acceleration event of the 6MW was verified manually. A threshold was manually adjusted (by ensuring exactly one peak passes the threshold in each gait cycle for each ankle) to identify initial swing peaks from the sagittal acceleration signal of both ankles. The adjustable thresholds are chosen manually for each segment of active data in which events can be reliably identified. The segment start and end are chosen manually so that only data in which peaks are identified correctly based on the peak thresholds is included. Any peaks that are not automatically detected or are detected incorrectly are manually identified or corrected individually.

The peak detection function is taken directly from LabVIEW; it is given only the threshold-passing points. We used a quadratic fit over 8 samples to identify each peak. After manually verifying and identifying additional peaks if needed, the expert rater checks that the number of peaks identified from the right ankle is equal to that identified from the left ankle for each segment of events. If the location within the gait cycle corresponding to a peak is unclear, it is omitted from the ground truth data. In general, the first large peak of the gait cycle is taken as the event; although in a small subset of the trials ($\frac{8}{98}$), a slightly different location, such as the trough (corresponding to heel impact), was chosen

for better consistency from one gait cycle to the next. For these trials, one or both of the ankle sagittal acceleration signals were inverted before manually identifying peaks using the LabVIEW program. They were also inverted before applying any of the gait event identification algorithms.

The GT event identification was also verified in MATLAB by a second expert rater, plotting the right ankle and left ankle signals individually along with the corresponding events identified in the LabVIEW program; any mistakes in the event identification were again fixed manually.

The ground truth processing provides sample numbers corresponding to the segment starts, segment ends, peaks identified from the left ankle sagittal acceleration signal, and peaks identified from the right ankle sagittal acceleration signal. However, originally, the segment starts and ends are not very meaningful – they correspond to the starts and ends of segments for which a common threshold was selected. Therefore, if the first GT peak of an original segment start was less than 1.5 times the average cycle length (calculated from the differences between consecutive GT peaks within all the original segments) following the last GT peak of an original segment end, these original segment markers were deleted.

The period of time between a processed segment start and corresponding segment end represents a period in which manual events were consistently identified. Therefore, the final segments are representative of the ground truth activity. These segment starts and ends are forced to occur one third of the average cycle length before and after the first and last event of the GT active segment, respectively. The average cycle length is determined by taking the average of the difference between the peaks from one ankle across all segments.

We define segments as periods in which GT events were consistently identified. Manually identified events occurring in segments containing three or fewer peaks per ankle were discarded.

5.2 Results

The proposed method is compared to GT data to assess the accuracy of the algorithm's estimated phase at each GT event, the ratio of the number of estimated events to the number of GT events, the F1 score, and the number of gait cycles it takes to meet the ratio convergence criteria. We further assess our proposed method by comparing it to existing peak detection methods.

5.2.1 Performance Analysis Metrics

Each implementation (using different learning rates) is evaluated. This includes the default learning rates, the learning rates optimized on a set of training data, and the learning rates optimized for each test trial individually (Section 5.1.4).

Table 5.2 provides the evaluated metrics: phase error (PE), events ratio (ER), F1 score, convergence time (CT), and the percentage of segments converged.

Note, phase error can be calculated even when the model does not satisfy convergence criteria (*e.g.,* when the model is active but not converged and ratio convergence criteria have previously been met). For this reason, we also analyze converged phase error (CPE), which evaluates only phase error associated with GT events in which the model meets convergence criteria.

If there are many more or many fewer estimated events compared to GT events, the model has not been learned correctly (ω is too high or too low, respectively). The ratio of estimated events and GT events is important since low PE is possible if the model has high frequency and the phase is changing rapidly.

In [14], a metric for evaluating motion segmentation algorithms is proposed. We use their Integrated Kernel method to evaluate the F1 score, where we set the standard deviation of the Gaussian associated with each estimated and GT event to be one quarter of the GT gait cycle length (*i.e.* 95% of the Gaussian is within one quarter of the GT gait cycle length of the event).

For the CT metric, both the initial convergence time (iCT) and the mean of all following (pre-learned) convergence times (pCT) are recorded to distinguish any effects from the model already having been learned.

5.2.2 Performance Analysis Results

Table 5.3 shows the phase error, the converged phase error, the ratio of the number of estimated events to the number of GT events, the F1 scores, the convergence times, and the percentage of active segments that met convergence criteria when using analytical event identification. The ideal phase error and convergence time is 0 while the ideal events ratio and F1 score is 1, and the ideal percentage converged is 100. The mean ($\pm$ standard deviation) is shown for each performance measure, across all trials.

The results show good performance for all metrics. The best results were obtained using individually optimized learning rates but performance decreases only slightly using

Table 5.2: Performance Metrics

Metric	Expression	Description
PE	$\frac{1}{E}\sum_{i=1}^{E}\lvert PO_i\rvert$	Mean absolute value of the PO (see Section 5.1.4) over all GT events after convergence criteria have initially been met
ER	$\frac{\#Estimated\ Events}{\#GT\ Events}$	Ratio of estimated events and GT events (defined in Section 5.1.4)
F1	As defined in [14] using a standard deviation of one quarter of the GT gait cycle length	Measure of how closely the estimated events coincide with the GT events
CT[a]	$\frac{\sum_{i=1}^{C} t_{ci}-t_{ai}}{GT\ Cycle\ Length}$	Gait cycles passed before the estimated gait model meets the convergence criteria once the signal has been deemed active
Converged	$\frac{\#Converged\ GT\ Segments}{\#GT\ Segments}$	Percentage of active segments containing more than five gait cycles which meet convergence criteria

[a] Note, iCT evaluates $i = 1$ and pCT evaluates $i = 2 \rightarrow C$

Table 5.3: Performance measures for faller and non-faller groups using analytical event identification, relative to learning rate selection. Phase error values are shown as a percentage of the GT gait cycle length; ER and F1 are ratios in which 1 is ideal; and convergence times are shown as a multiple of GT gait cycles, where the first term is the initial convergence time and the second is the prelearned convergence time. Each measure shows the mean and standard deviation across all trials.

Learning Rates (μ, η)	**PE (%)**	**CPE (%)**	**ER**	**F1**	**iCT**	**pCT**	**Converged (%)**
Default (0.01, 1)	**4 (±4)**	**3 (±4)**	**0.99 (±0.10)**	**0.91 (±0.11)**	**9.36 (±8.00)**	**7.33 (±6.52)**	**96.83 (±12.16)**
Fallers	4 (±4)	3 (±3)	0.98 (±0.14)	0.90 (±0.11)	9.35 (±7.45)	8.12 (±7.72)	95.85 (±15.73)
Non-Fallers	3 (±4)	3 (±5)	1.00 (±0.02)	0.92 (±0.11)	9.36 (±8.57)	6.58 (±5.11)	97.78 (±7.33)
Group Optimized (0.01, 2.30)	**4 (±5)**	**3 (±5)**	**1.00 (±0.01)**	**0.90 (±0.13)**	**4.13 (±2.35)**	**3.67 (±2.99)**	**99.20 (±5.72)**
Fallers	5 (±6)	4 (±5)	1.00 (±0.02)	0.88 (±0.13)	4.07 (±2.32)	4.13 (±3.92)	98.37 (±8.14)
Non-Fallers	3 (±5)	3 (±5)	1.00 (±0.01)	0.91 (±0.12)	4.18 (±2.40)	3.21 (±1.59)	100.00 (±0.00)
Individually Optimized (μ^*, η^*)	**3 (±4)**	**3 (±3)**	**1.00 (±0.02)**	**0.90 (±0.11)**	**4.89 (±5.79)**	**3.12 (±3.50)**	**99.04 (±8.02)**
Fallers	4 (±4)	3 (±4)	1.01 (±0.02)	0.89 (±0.12)	4.90 (±6.60)	3.40 (±4.22)	98.38 (±11.23)
Non-Fallers	3 (±3)	3 (±3)	1.00 (±0.02)	0.92 (±0.09)	4.88 (±4.97)	2.85 (±2.62)	99.67 (±2.36)

default or group optimized learning rates. Note that the results shown in Table 5.3 are for the test set of trials and were not used during parameter selection. We see the algorithm works for both fallers and non-fallers, without significant differences, indicating that the method works well for a variety of gaits and conditions.

The ER is close to one and the percentage of segments which met convergence criteria is close to 100% for all three implementations. When using analytical event identification, there is an average phase error of 4% and an average F1 score of 0.90. For the optimized learning rates, the gait model is learned in approximately four strides when there is no a priori knowledge about gait parameters and slightly faster when a previous model is available. The most significant difference in performance with respect to the learning rates are the convergence times, which are about twice as long when using the default learning rates.

Note, the PE and CPE measures are not significantly different from one another, indicating performance does not suffer significantly when the model has not yet met convergence criteria. This indicates that a representative gait model is learned quickly. We see this in Figure 3.2 where the phase of peak events does not change much from before to after convergence criteria have been met.

Table 5.4 shows the performance measures using the initial manual event identification method. The ER and percentage of segments converged have similar performance, whereas the phase error, F1 score, and optimized convergence times are worse than the analytical event identification. The average phase error is 7% and the average F1 score is 0.83. The convergence times are best using the individually optimized learning rates, followed by the group optimized learning rates, and then the default learning rates; for the group optimized learning rates the iCT is approximately 7 strides and the pCT is approximately 6 strides. The default learning rates produce similar convergence times to those found when using the analytical event identification. Note that the metrics vary considerably more with respect to the learning rates when using initial event identification.

The same analysis was run on the right ankle data, with similar results for each metric and each learning rate selection relative to the event identification implementation.

5.2.3 Comparison to Peak Detection Methods

The majority of existing algorithms in the literature are based on thresholds or peak detection [39], [73], [72], [38], [56], [67], [30], [11], [10]. Unfortunately, almost all implementations require a specific type of input signal. Further, many cannot be implemented in real-time [38], [29], [3], [2].

Table 5.4: Performance measures for faller and non-faller groups using initial manual event identification, relative to learning rate selection. Phase error values are shown as a percentage of the GT gait cycle length; ER and F1 are ratios in which 1 is ideal; and convergence times are shown as a multiple of GT gait cycles, where the first term is the initial convergence time and the second is the prelearned convergence time. Each measure shows the mean and standard deviation across all trials.

Learning Rates (μ, η)	**PE (%)**	**CPE (%)**	**ER**	**F1**	**iCT**	**pCT**	**Converged (%)**
Default (0.01, 1)	**7 (±6)**	**6 (±5)**	**1.00 (±0.11)**	**0.82 (±0.14)**	**9.27 (±7.66)**	**7.62 (±6.40)**	**96.55 (±11.05)**
Fallers	7 (±6)	6 (±5)	0.99 (±0.15)	0.82 (±0.15)	8.87 (±6.55)	8.39 (±7.61)	95.79 (±13.57)
Non-Fallers	7 (±6)	6 (±6)	1.01 (±0.05)	0.82 (±0.13)	9.65 (±8.64)	6.87 (±4.92)	97.28 (±8.00)
Group Optimized (0.01, 1.65)	**7 (±6)**	**6 (±6)**	**1.01 (±0.05)**	**0.82 (±0.14)**	**7.06 (±11.82)**	**5.56 (±4.12)**	**97.89 (±8.03)**
Fallers	7 (±6)	7 (±6)	1.02 (±0.05)	0.80 (±0.15)	5.88 (±5.20)	6.28 (±5.32)	97.11 (±10.17)
Non-Fallers	6 (±6)	6 (±6)	1.01 (±0.05)	0.83 (±0.14)	8.19 (±15.75)	4.87 (±2.37)	98.63 (±5.26)
Individually Optimized (μ^*, η^*)	**6 (±4)**	**5 (±4)**	**1.01 (±0.02)**	**0.84 (±0.10)**	**5.60 (±5.97)**	**4.29 (±3.21)**	**98.91 (±6.30)**
Fallers	6 (±5)	5 (±5)	1.01 (±0.02)	0.83 (±0.11)	4.60 (±4.36)	4.28 (±3.50)	98.84 (±8.02)
Non-Fallers	5 (±4)	5 (±4)	1.01 (±0.02)	0.85 (±0.09)	6.56 (±7.10)	4.31 (±2.93)	98.98 (±4.12)

Table 5.5: Heuristic Event Identification Performance Measures

Algorithm	F1	ER
Peak Detection with Prior	0.84 (±0.08)	0.84 (±0.13)
Threshold (1000)	0.76 (±0.19)	1.32 (±0.57)
Threshold (1400)	0.68 (±0.25)	0.98 (±0.55)
Billauer [7]	0.71 (±0.11)	1.83 (±0.50)
Proposed – Analytical Default	0.90 (±0.10)	0.99 (±0.10)

We compared the performance of three online peak detection implementations for identifying initial swing events: one with prior knowledge of gait speed and two without. The F1 score and ER were evaluated for all trials in which initial swing events were identified.

The first implementation assumes that the gait cycle is approximately one second long and greater than 0.5 seconds long. Each time the estimated gait cycle length has passed, the maximum value in the previous gait cycle is taken to be the event (similar to [3] and [28]). The estimated gait cycle length is updated to be the mean of the one second initialization along with all differences between previous contiguous events that are greater than 0.5 seconds. Results are shown in the first row of Table 5.5. We see the events ratio is significantly smaller than the analytical event identification implementation using default learning rates (shown in the bottom row).

The second implementation uses MATLAB's *findpeaks* function with the "MinPeakHeight" specification, specifying a threshold that must be exceeded to identify a peak (similar to the footswitch force threshold algorithm in [21]). In the second and third rows of Table 5.5, we show results for two thresholds, one which generates the best F1 score (1000) and the other which generates the best ER score (1400). Here we see significantly lower F1 scores for both thresholds and one ER score which is significantly larger than 1.

The last implementation is a real-time peak detection algorithm provided by [7] (also used as a baseline in [29]). Local maxima and minima are searched for alternately, such that the identified maxima/minima is δ greater than or less than the previously identified minima/maxima. We set $\delta = 1000$; the results are shown in the fourth row of Table 5.5. With this implementation, we often see multiple peaks identified per gait cycle, since the maxima and minima are often very far apart for multiple maxima within a single gait cycle.

5.3 Summary

We implement the proposed approach on a gait dataset taken from a group of retirement home residents who each have a variety of medical conditions, measuring ankle sagittal linear acceleration. The ground truth identification of initial swing events are identified with the help of a program which allows each event to be verified manually. Using the analytical event identification method and the default learning rates, the proposed approach converges within approximately eight gait cycles and initial swing events are extracted with an average error of 0.03 gait cycles. When using learning rates optimized on a set of training trials, the proposed approach converges within approximately four gait cycles and maintains an average error of 0.03 gait cycles, on the corresponding set of test trials. Further, when including ground truth events occurring prior to the model having met convergence criteria, the average error is only slightly increased to 0.04 gait cycles. The initial manual event identification method has greater error than the analytical event identification method, with an average absolute error of approximately 0.06 gait cycles when using group optimized or default learning rates.

Chapter 6

Discussion and Conclusions

This chapter discusses the strengths and limitations of the proposed approach. In particular, we discuss the choice of event identification method, the choice of optimization weights, a comparison to related work, limitations when applying the proposed approach to an arbitrary gait signal and on gait model learning, as well as real-time processing requirements for various applications. We then summarize the main conclusions and future work.

6.1 Discussion

The proposed algorithm works accurately and in real-time without prior knowledge of the gait signal. While learning rates can be optimized to improve performance, the set of default learning rates can be used with only a small decrease in performance. In general, if the learning rates are smaller, it will take longer for the model to be learned.

6.1.1 Event Identification Method

When we know the properties of the events to identify, we can use the analytical event identification method, which addresses both initial manual event identification weaknesses: it is completely automated and has better performance since we update the event phase each cycle based on any changes in the gait model.

The initial manual event identification method demonstrates that all events can be identified with the help of a labeller for only a single event, still saving a significant amount

of time. However, if the gait and the corresponding gait model change over time, we may also see a slight change in the event phase over time. The analytical event identification method can be used if the event signal characteristics necessary to develop initial heuristic event identification are known. This method has better performance since the event phase is updated each cycle based on any changes in the gait model.

The analytical event identification method's performance is good even before convergence criteria are met since the event identification improves gradually as the model is learned. This means that it is not as dependent on the measures of convergence times. On the other hand, the initial event identification method is only permitted to update the event phase after convergence criteria have been met to ensure the phase is correct and thus has decreased accuracy when convergence criteria are made more lenient.

6.1.2 Choice of Optimization Weights

In this thesis, J_{PO} and J_{ER} have the highest weight settings since the main goal is to reduce the PO at each GT event, while also ensuring the model is learned. We also desire fast convergence time, but if the weight of J_{CT} is too high, the magnitude of the selected learning rates also become too high, which can lead to unstable performance in some trials. The learned model should be a close approximation of the input signal; however, J_e does not need to be too small, as the model can still be an accurate representation without zero error.

Our learning rate optimization captures a variety of evaluation criteria, which may be of differing importance in specific applications. For example, the current weights balance between reduced convergence times and reduced phase error. If convergence time was not an issue (*e.g.,* for long duration walking data), the convergence weight could be reduced.

Note that in Table 5.3 when using the group optimized learning rates, the fallers have larger pCT than iCT. In the current optimization, iCT and pCT have the same weights so it makes sense that they would be closer when using these optimized learning rates. Also, the faller data has more variability, hence saving a prelearned model would not be as helpful as with the non-faller data.

6.1.3 Comparison to Related Work based on Temporal Error

To enable comparison to works in the literature that do not consider gait periodicity, we also computed the time offset error for the analytical event identification applied to the

older adult dataset. There was an average absolute error of 32.8 (± 56.5) milliseconds and 39.1 (± 65.9) milliseconds between each converged estimated event and the nearest ground-truth event, when using the default and group optimized learning rates, respectively.

However, many papers, including [28],[47],[41], [18], report the average error, as opposed to the average absolute error. For our method, the average error is -2.1 (± 30.7) milliseconds when using the default learning rates and 5.6 (± 70.6) milliseconds when using the group optimized learning rates, between each converged estimated event and the nearest ground truth event. Note, a negative error means the nearest ground truth event occurred before the estimated event. The corresponding 95% confidence interval for the mean difference between estimated and ground truth events per trial (each containing 300 converged estimated events on average) was within 2.7 milliseconds using the default learning rates and within 19.4 milliseconds using the group optimized learning rates.

The implemented group optimized learning rates are slightly less accurate for event identification but meet convergence criteria much more quickly. This tradeoff can be adjusted in the choice of optimization weights, discussed in Section 6.1.2.

The temporal error performance matches or exceeds most of the related work which evaluate event identification [28], [41], [47], [3], [18]. Hanlon and Anderson [21] report lower average absolute error, but their implementation requires two accelerometers (one at the ankle and one at the knee) which have sampling rates of 1000 Hz. Training and test data were collected in the same controlled environment, with the same ground surface and accelerometer attachment sites, from twelve healthy participants. 41 accelerometer event identification algorithms were developed based on the training dataset and they report the best results of all these algorithms when applied to the test dataset.

The proposed approach is competitive with the existing methods, but a direct comparison is difficult because of the differing datasets, sensor suites, and sampling rates. Note that for our approach, the data was collected at 40-50 Hz before being upsampled to 100 Hz.

6.1.4 Limitations

The main limitations are the possible dependency on the use of a specific gait signal for the activity recognition, the convergence criteria, and the event identification as well as the convergence time required by the algorithm.

Specific Input Signal

The current activity recognition approach is based on a simple signal-dependent heuristic. It uses a threshold, T_a, which the standard deviation across the previous window of input, σ_t, must surpass to initially identify activity. The choice of threshold depends on the amplitude of the specific input gait signal. The threshold for the error convergence criteria, T_{ce}, is similarly dependent on the specific input gait signal. The ratio convergence criteria is less dependent on a specific input gait signal since it compares the ratio of the average absolute input signal to the average absolute estimated signal, but this should be validated on a larger number of gait signals.

Although the method was directly transferrable from the young adult dataset (using gyroscope data) to the older adult dataset (using accelerometer data), a few changes were made. The most important change was the increase in the number of harmonics, M, for the Fourier series gait model representation to capture the higher frequency components introduced by accelerometer data. However, this could be updated online based on the frequency components contained in the input signal.

A limitation of the proposed approach is that it does not explicitly identify specific gait events (*i.e.*, foot strike or toe off); these must be manually associated with a particular phase value or signal characteristics. This is undesirable since event signal characteristics are often dependent on the specific input signal which is used. Further, signal characteristics used to identify a particular gait event in a healthy population may not be suitable for identification of the same gait event in an unhealthy population. Therefore, to apply gait event identification to an arbitrary input gait signal, signal invariant gait event characteristics would need to be identified. Alternatively, manual initial event identification can be used, where manual labels are required in the first converged gait cycle.

Convergence Time

Another limitation is the time required to learn the gait model (*i.e.* the gait model is not known instantaneously). While the analytical event identification had good performance even before convergence criteria were met, initial event identification requires a manual label during the first converged gait cycle and therefore is not able to identify gait events before convergence criteria are met without a reduction in gait event identification accuracy. Since only a few steps are available for some ambulatory monitoring tasks, initial event identification may not be applicable for these cases.

6.1.5 Application Dependent Real-Time Requirements

Gait event identification is used in many applications, such as fall risk assessment [44], [60], biometrics [17], [13], [12], health characterization [1], localization [30, 34, 22, 11], and control of assistive devices such as prostheses [42], [19], exoskeletons [31], and functional electrical stimulation devices [59, 55, 58]. However, the amount of acceptable delay is dependent on the specific application. For example, gait event identification for the control of gait assistive devices should not be delayed more than 100 to 125 ms for optimal performance [16]. While implementations with significant delay in processing are still useful for many applications, the smaller the delay, the better. For example, the sooner feedback (such as risk of fall or disease) from health monitoring devices can be provided, the more likely this information can be used to prevent or mitigate possible future health problems.

While the event identification for the proposed approach requires very little computation, the amount of delay added will depend on the device hardware which is selected for the chosen application. If the initial event identification method is chosen, event identification will be initially delayed by the convergence time; whereas we saw good performance for the analytical event identification method even before convergence criteria had been met. Also, if a larger window length, wl, is chosen, there would be a delay in recognizing activity (and consequently, beginning to learn the gait model) as well as determining that the gait model has been learned. Therefore, the hardware, settings, and methods should be chosen with respect to the specific application.

6.2 Conclusions

The proposed method generates an accurate, individualized model of gait that can be used to estimate gait events in real-time. The phase can also be used to accurately align multiple strides, providing both a measure of the gait parameters and their variability, a key measure of interest in gait analysis [23], [6].

Two methods of gait event identification were implemented: analytical event identification and initial event identification. Three methods of selecting learning rates were analyzed: using a default set of learning rates, using the learning rates selected by an optimization performed on a representative group of training trials, and using the learning rates selected by an optimization on each test trial.

We obtained good performance for all metrics. For the young adult dataset, the proposed approach converges within approximately five gait cycles and heel impact and toe

takeoff events are extracted with an average absolute error of 0.04 gait cycles, using the manual initial event identification method with default learning rates.

For the older adult dataset, the proposed approach converges within approximately eight gait cycles and initial swing events are extracted with an average error of 0.03 gait cycles, using the analytical event identification method with default learning rates. When using learning rates optimized on a set of training trials, the proposed approach converges within approximately four gait cycles and maintains an average error of 0.03 gait cycles, on the corresponding set of test trials. Further, when including ground truth events occurring prior to the model having met convergence criteria, the average error is only slightly increased to 0.04 gait cycles. The initial manual event identification method has worse performance but still converges within approximately seven gait cycles and initial swing events are extracted with an average error of 0.06 gait cycles when using group optimized learning rates.

6.3 Future Work

In the future, we plan to implement an alternate evaluation approach; implement online parameter adaptation; apply the proposed approach to combinations of inputs and use a multivariate gait model representation; implement gait recognition so that gait from a constant stream of data can be monitored; use prior knowledge to explicitly identify specific gait events; and report user diagnostics.

6.3.1 Alternate Evaluation Approach

We would like to further evaluate our method by comparing gait parameters, such as step time variability, computed from the GT event data and from the estimated event data. These additional gait parameter performance metrics would more explicitly define the applicability of the proposed approach in understanding fall risk.

6.3.2 Online Parameter Adaptation

We would like to further explore adapting/selecting other algorithm parameters in real-time. Incremental updates could be made to the learning rates based on the gait input signal. For example, when the input is determined to be gait but has not yet met convergence criteria, we want higher learning rates; whereas when the gait has met convergence

criteria, learning rates could be lowered. This would help with decreasing convergence times and improving accuracy of the event identification.

Further, we would like to investigate adapting/selecting the number of harmonics, M, to be used in the model representation, based on the gait input signal. The more frequency components in the input signal, the larger the model number of harmonics should be to capture these details. This could be evaluated online and updated accordingly.

6.3.3 Multivariate Gait Model

In this implementation, we have discarded the other accelerometer/gyroscope axes and accelerometers/IMUs because only one signal is necessary to determine the phase of the gait cycle; once this phase is learned, it can be applied to all measured signals. Alternatively, the gait model could be formulated as a multivariate model in which the frequency and phase are synchronized between channels. A multivariate gait model could be used when there are multiple input signals (*i.e.* inertial measurement units are often placed at multiple locations and each collect linear acceleration and angular velocity along three axes), in which the frequency and phase are synchronized but the coefficients are specific to each input source. This model would incorporate more information, likely creating a more robust and accurate gait model representation.

6.3.4 Gait Recognition

In the long term, we would like to be able to run the algorithm continuously, collecting a constant stream of data for full-day health monitoring. This would be especially useful to those at greater risk of fall/disease, and is very feasible with the recent advances in micro-electromechanical systems (MEMS) IMU sensors, which provide a continuous measure of linear acceleration and angular velocity.

In this case, we would need to implement gait recognition, as opposed to just activity recognition. The current activity recognition only distinguishes between gait and non-gait data, which mainly includes pauses, breaks, and turns. If we apply the algorithm to constantly monitor someone's gait, we will need to be able to distinguish gait from a much larger number of activities, some of which may resemble gait quite closely.

6.3.5 Prior Gait Knowledge

The current implementation does not explicitly identify specific gait events (*i.e.* foot strike or toe off); these must be manually associated with signal characteristics or a particular phase value. We would like to combine our prior knowledge about gait and what we find to be common across models from a variety of individuals and measurement signal types with the individualized model we learn in real-time, to identify specific gait events without needing to provide associated gait event signal characteristics.

6.3.6 Diagnostics

We would like to perform subsequent analysis investigating how the learned gait models are related or indicative of various diseases or risk of fall. Since our dataset also consists of a large number of demographics, we could first evaluate which demographic information best predicts model parameters. We could then use the model parameters to evaluate the prediction of various diseases and fall. These could be implemented using least absolute shrinkage and selection operator (LASSO), which performs both variable selection and regularization, using regression. This could be used to update users and care-givers in real-time when users are at increased risk for fall or disease.

Additionally, we would like to investigate whether the learned model parameters are directly interpretable for clinical use. For example, if the Fourier coefficients are related to impact amplitude, this could be useful for shoe evaluation or osteoporosis.

References

[1] Murad Alaqtash, Huiying Yu, Richard Brower, Amr Abdelgawad, and Thompson Sarkodie-Gyan. Application of wearable sensors for human gait analysis using fuzzy computational algorithm. *Engineering Applications of Artificial Intelligence*, 24:1018–1025, 2011.

[2] K. Aminian, B. Najafi, C. Büla, P.-F. Leyvraz, and Ph. Robert. Spatio-temporal parameters of gait measured by an ambulatory system using miniature gyroscopes. *Journal of Biomechanics*, 35(5):689–699, 2002.

[3] K Aminian, K Rezakhanlou, I E De Andres, C Fritsch, P.-F Leyvraz, and P Robert. Temporal feature estimation during walking using miniature accelerometers: an analysis of gait improvement after hip arthroplasty. *Med. Biol. Eng. Comput*, 37:686–691, 1999.

[4] The Canadian Medical Association. Health and Health Care for an Aging Population Policy Summary of The Canadian Medical Association Health and Health Care for an Aging Population. 2013.

[5] Min S H Aung, Sibylle B. Thies, Laurence P J Kenney, David Howard, Ruud W. Selles, Andrew H. Findlow, and John Y. Goulermas. Automated detection of instantaneous gait events using time frequency analysis and manifold embedding. *IEEE Transactions on Neural Systems and Rehabilitation Engineering*, 21(6), 2013.

[6] C. K. Balasubramanian, R. R. Neptune, and S. A. Kautz. Variability in spatiotemporal step characteristics and its relationship to walking performance post-stroke. *Gait Posture*, pages 408–414, 2009.

[7] Eli Billauer. peakdet: Peak detection using matlab. http://www.billauer.co.il/peakdet.html. Last updated: 2012. Accessed: 2018.

[8] Dustin A Bruening and Sarah Trager Ridge. Automated event detection algorithms in pathological gait. *Gait & Posture*, 39:472–477, 2014.

[9] Jonas Buchli, Ludovic Righetti, and Auke Jan Ijspeert. A Dynamical Systems Approach to Learning : A Frequency-Adaptive Hopper Robot. *Dynamical Systems*, (c):210–220, 2005.

[10] Nadir Castañeda and Sylvie Lamy-Perbal. An improved shoe-mounted inertial navigation system. *2010 International Conference on Indoor Positioning and Indoor Navigation, IPIN 2010 - Conference Proceedings*, (September):15–17, 2010.

[11] Filippo Cavallo, Angelo M. Sabatini, and Vincenzo Genovese. A step toward GPS/INS personal navigation systems: Real-time assessment of gait by foot inertial sensing. *2005 IEEE/RSJ International Conference on Intelligent Robots and Systems, IROS*, pages 109–113, 2005.

[12] David Cunado, Mark S Nixon, and John N Carter. Automatic extraction and description of human gait models for recognition purposes.

[13] Mohammad Omar Derawi. Accelerometer-Based Gait Analysis, A survey.

[14] Christian R G Dreher, Nicklas Kulp, Christian Mandery, Mirko Wächter, and Tamim Asfour. A Framework for Evaluating Motion Segmentation Algorithms. *IEEE-RAS International Conference on Humanoid Robots (Humanoids)*, 2017.

[15] Andreas Ejupi, Stephen R. Lord, and Kim Delbaere. New methods for fall risk prediction. *Current Opinion in Clinical Nutrition and Metabolic Care*, 17(5):407–411, 2014.

[16] Todd R. Farrell and Richard F. Weir. The optimal controller delay for myoelectric prostheses. *IEEE Transactions on Neural Systems and Rehabilitation Engineering*, 15(1):111–118, 2007.

[17] J L Geisheimer, W S Marshall, and E Greneker. A continuous-wave (CW) radar for gait analysis. *Conference Record of ThirtyFifth Asilomar Conference on Signals Systems and Computers CatNo01CH37256*, 1:834–838, 2001.

[18] Rafael C González, Antonio M López, Javier Rodriguez-Uría, Diego Avarez, and Juan C Alvarez. Real-time gait event detection for normal subjects from lower trunk accelerations. pages 322–325, 2010.

[19] Maja Goršič, Roman Kamnik, Luka Ambrožič, Nicola Vitiello, Dirk Lefeber, Guido Pasquini, and Marko Munih. Online phase detection using wearable sensors for walking with a robotic prosthesis. *Sensors (Switzerland)*, 14(2):2776–2794, 2014.

[20] J. Green, A. Forster, and J. Young. Reliability of gait speed measured by a timed walking test in patients one year after stroke. *Clin Rehabil.*, 16:306–314, 2002.

[21] Michael Hanlon and Ross Anderson. Real-time gait event detection using wearable sensors. *Gait & Posture*, 30(4):523–527, 2009.

[22] Robert Harle. A Survey of Indoor Inertial Positioning Systems for Pedestrians. 15(3):1281–1293, 2013.

[23] J. M. Hausdorff. Gait variability: methods, modeling and meaning. *J. NeuroEng. Rehabil.*, 2005.

[24] Jeffrey M. Hausdorff, Dean A. Rios, and Helen K. Edelberg. Gait variability and fall risk in community-living older adults: A 1-year prospective study. *Archives of Physical Medicine and Rehabilitation*, 82(8):1050–1056, 2001.

[25] Wan He, Daniel Goodkind, and Paul Kowal. An Aging World: 2015. 2016.

[26] Alan Hreljac and Robert N Marshall. Algorithms to determine event timing during normal walking using kinematic data. *Journal of Biomechanics*, 33:783–786, 2000.

[27] Irvin Hussein López-Nava and Angélica Muñoz-Meléndez. Towards Ubiquitous Acquisition and Processing of Gait Parameters. 2010.

[28] Jan M Jasiewicz, John H J Allum, James W Middleton, Andrew Barriskill, Peter Condie, Brendan Purcell, Raymond Che, and Tin Li. Gait event detection using linear accelerometers or angular velocity transducers in able-bodied and spinal-cord injured individuals. 2006.

[29] Shuo Jiang, Xingchen Wang, Maria Kyrarini, and Axel Gräser. A Robust Algorithm for Gait Cycle Segmentation. pages 31–35, 2017.

[30] A. R. Jiménez, F. Seco, C. Prieto, and J. Guevara. A comparison of pedestrian dead-reckoning algorithms using a low-cost MEMS IMU. *WISP 2009 - 6th IEEE International Symposium on Intelligent Signal Processing - Proceedings*, pages 37–42, 2009.

[31] Chetas D. Joshi, Uttama Lahiri, and Nitish V. Thakor. Classification of gait phases from lower limb EMG: Application to exoskeleton orthosis. *IEEE EMBS Special Topic Conference on Point-of-Care (POC) Healthcare Technologies: Synergy Towards Better Global Healthcare, PHT 2013*, pages 228–231, 2013.

[32] Vladimir Joukov, Vincent Bonnet, Michelle Karg, Gentiane Venture, and Dana Kulic. Rhythmic Extended Kalman Filter for Gait Rehabilitation Motion Estimation and Segmentation. *IEEE Transactions on Neural Systems and Rehabilitation Engineering*, 2017.

[33] Siddhartha Khandelwal; and Nicholas Wickstrom;. Identification of Gait Events using Expert Knowledge and Continuous Wavelet Transform Analysis. *Harald Loose, Guy Plantier, Tanja Schultz, Ana Fred & Hugo Gamboa (ed.), BIOSIGNALS 2014: Proceedings of the International Conference on Bio-inspired Systems and Signal Processing*, (Biosignals):197–204, 2014.

[34] Jeong Won Kim, Han Jin Jang, Dong-Hwan Hwang, and Chansik Park. A Step, Stride and Heading Determination for the Pedestrian Navigation System. *Journal of Global Positioning Systems*, 3(12):273–279, 2004.

[35] Richard T. Lauer, Brian T. Smith, and Randal R. Betz. Application of a neuro-fuzzy network for gait event detection using electromyography in the child with cerebral palsy. *IEEE Transactions on Biomedical Engineering*, 52(9):1532–1540, 2005.

[36] Seon-Woo Lee, Kenji Mase, and Kiyoshi Kogure. Detection of spatio-temporal gait parameters by using wearable motion sensors. *Conference proceedings : ... Annual International Conference of the IEEE Engineering in Medicine and Biology Society. IEEE Engineering in Medicine and Biology Society. Conference*, 7:6836–9, 2005.

[37] David Levine, Jim Richards, and Michael W. Whittle. *Whittle's Gait Analysis*. 2012.

[38] P. Lopez-Meyer, G. D. Fulk, and E. S. Sazonov. Automatic detection of temporal gait parameters in poststroke individuals. *IEEE Trans. Inf. Technol. Biomed.*, 15(4):594–601, 2011.

[39] I. H. López-Nava and A. Muñoz-Meléndez. Towards ubiquitous acquisition and processing of gait parameters. *MICAI*, pages 410–421, 2010.

[40] B E Maki. Gait changes in older adults: predictors of falls or indicators of fear. *Journal of the American Geriatrics Society*, 45(3):313–320, 1997.

[41] A. Mannini, D. Trojaniello, U. D. Croce, and A. M. Sabatini. Hidden markov model-based strategy for gait segmentation using inertial sensors: Application to elderly, hemiparetic patients and huntington's disease patients. *Conf Proc IEEE Eng Med Biol Soc.*, pages 5179–5182, 2015.

[42] Hafiz Farhan Maqbool, Muhammad Afif Bin Husman, Mohammed I. Awad, Alireza Abouhossein, Nadeem Iqbal, and Abbas A. Dehghani-Sanij. A Real-Time Gait Event Detection for Lower Limb Prosthesis Control and Evaluation. *IEEE Transactions on Neural Systems and Rehabilitation Engineering*, 25(9):1–1, 2016.

[43] Benoit Mariani, Hossein Rouhani, Xavier Crevoisier, and Kamiar Aminian. Quantitative estimation of foot-flat and stance phase of gait using foot-worn inertial sensors. *Gait and Posture*, 2013.

[44] Michael Marschollek, A. Rehwald, K. H. Wolf, M. Gietzelt, G. Nemitz, H. Meyer zu Schwabedissen, and R. Haux. Sensor-based fall risk assessment - an expert 'to go'. *Methods of Information in Medicine*, 50(5):420–426, 2011.

[45] S. J. Marshall, S. S. Ley, C. E. Tudor-Locke, F. W. Kolkhorst, K. M. Wooten, M. Ji, C. A. Macera, and B. E. Ainsworth. Translating physical activity recommendations into a pedometer-based step goal. *Am. J. Prev. Med.*, 36(5):410–415, 2009.

[46] Hylton B Menz, Mark D Latt, Anne Tiedemann, Marcella Mun San Kwan, and Stephen R Lord. Reliability of the GAITRite® walkway system for the quantification of temporo-spatial parameters of gait in young and older people. *Gait & Posture*, 20(1):20–25, 2004.

[47] A. Miller. Gait event detection using a multilayer neural network. *Gait Posture*, 29:542–545, 2009.

[48] Sau Kuen Ng and Howard Jay Chizeck. Fuzzy model identification for classification of gait events in paraplegics. *IEEE Transactions on Fuzzy Systems*, 5(4):536–544, 1997.

[49] E. Nordin, N. Lindelöf, E. Rosendahl, J. Jensen, and L. Lundin-Olsson. Prognostic validity of the timed up-and-go test, a modified get-up-and-go test, staff's global judgement and fall history in evaluating fall risk in residential care facilities. *Age Ageing*, 37(4):442–448, 2008.

[50] E. Nordin, E Rosendahl, and L. Lundin-Olsson. Timed "up and go" test: Reliability in older people dependent in activities of daily living - focus on cognitive state. *Phys. Ther.*, 86(5):646–655, 2006.

[51] Public Health Agency of Canada. Seniors' Falls in Canada: Second Report.

[52] T. Petrič, A. Gams, A. J. Ijspeert, and L. Žlajpah. On-line frequency adaptation and movement imitation for rhythmic robotic tasks. *Int. J. Rob. Res.*, pages 1755–1788, 2011.

[53] L. Righetti, J. Buchli, and A. J. Ijspeert. Dynamic hebbian learning in adaptive frequency oscillators. *Physica D*, 216(2):269–281, 2006.

[54] K. R. Robertson, T. D. Parsons, J. J. Sidtis, T. H. Inmna, W. T. Robertson, C. D. Hall, and R. W. Price. Timed gait test: Normative data for the assessment of the aids dementia complex. *J. Clin. Exp. Neuropsychol.*, pages 1053–1064, 2006.

[55] Jan Rueterbories, Erika G. Spaich, Birgit Larsen, and Ole K. Andersen. Methods for gait event detection and analysis in ambulatory systems. *Medical Engineering & Physics*, 32(6):545–552, 2010.

[56] A. M. Sabatini, C. Martelloni, S. Scapellato, and F. Cavallo. Assessment of walking features from foot inertial sensing. *IEEE Trans. Biomed. Eng.*, 52(3):486–494, 2005.

[57] K. Salarian, A.; Russman, H.; Vingerhoets, F.; Dehollain, C.; Blanc, Y.; Burkhard, P.; Aminian. Gait Assessment in Parkinson's Disease: Toward an Ambulatory System for Long-Term Monitoring.

[58] Yoichi Shimada, Shigeru Ando, Toshiki Matsunaga, Akiko Misawa, Toshiaki Aizawa, Tsuyoshi Shirahata, and Eiji Itoi. Acceleration Sensor in FES Clinical Application of Acceleration Sensor to Detect the Swing Phase of Stroke Gait in Functional Electrical Stimulation. *Tohoku J. Exp. Med*, 207:197–202, 2005.

[59] Margaret M. Skelly and Howard Jay Chizeck. Real-time gait event detection for paraplegic FES walking. *IEEE Transactions on Neural Systems and Rehabilitation Engineering*, 9(1):59–68, 2001.

[60] D. A. Skelton, J. Kennedy, and O. M. Rutherford. Explosive power and asymmetry in leg muscle function in frequent fallers and non-fallers aged over 65. *Age Ageing*, 31:119–125, 2002.

[61] Dawn A. Skelton, Jonathon Kennedy, and Olga M. Rutherford. Explosive power and asymmetry in leg muscle function in frequent fallers and non-fallers aged over 65. *Age and Ageing*, 31(2):119–125, 2002.

[62] Brian T. Smith, Daniel J. Coiro, Richard Finson, Randal R. Betz, and James McCarthy. Evaluation of force-sensing resistors for gait event detection to trigger electrical stimulation to improve walking in the child with cerebral palsy. *IEEE Transactions on Neural Systems and Rehabilitation Engineering*, 10(1):22–29, 2002.

[63] Erik E. Stone and Marjorie Skubic. Unobtrusive, continuous, in-home gait measurement using the microsoft kinect. *IEEE Transactions on Biomedical Engineering*, 60(10):2925–2932, 2013.

[64] Philippe Terrier and Yves Schutz. How useful is satellite positioning system (GPS) to track gait parameters? A review.

[65] G. Thrane, R. M. Joakimsen, and E. Thornquist. The association between timed up and go test and history of falls: The tromsø study. *BMC Geriatr.*, 2007.

[66] Diana Trojaniello, Andrea Cereatti, Elisa Pelosin, Laura Avanzino, Anat Mirelman, Jeffrey M Hausdorff, and Ugo Della Croce. Estimation of step-by-step spatio-temporal parameters of normal and impaired gait using shank-mounted magneto-inertial sensors: application to elderly, hemiparetic, parkinsonian and choreic gait.

[67] Z. Wang and R. Ji. Estimate spatial-temporal parameters of human gait using inertial sensors. *IEEE-CYBER*, pages 1883–1889, 2015.

[68] J. L. S. Waugh, A. Trinh, R. R. Mohammed, W. E. McIlroy, and D. Kulić. Online learning of gait models for calculation of gait parameters. *IEEE EMBC*, pages 6146–6149, 2016.

[69] Jamie L. S. Waugh, Elaine Huang, Julia E. Fraser, Kit B. Beyer, Anton Trinh, William E. McIlroy, and D. Kulić. Online learning of gait models from older adult data. Submitted.

[70] Chao Yang, Zengyou He, and Weichuan Yu. Comparison of public peak detection algorithms for MALDI mass spectrometry data analysis. *BMC Bioinformatics*, 2009.

[71] J A Zeni, J G Richards, and J S Higginson. Two simple methods for determining gait events during treadmill and overground walking using kinematic data.

[72] H. Zhang, J. Zhang, D. Zhou, W. Wang, J. Li, F. Ran, and Y. Ji. Axis-exchanged compensation and gait parameters analysis for high accuracy indoor pedestrian dead reckoning. *J. Sensors*, 2015.

[73] S. Zhu, H. Anderson, and Y. Wang. A real-time on-chip algorithm for imu-based gait measurement. *Lect. Notes Comput. SC*, 7674:93 – 104, 2012.

[74] Shenggao Zhu, Hugh Anderson, and Ye Wang. A Real-Time On-Chip Algorithm for IMU-Based Gait Measurement. 2012.

APPENDICES

Appendix A

Analytical Peak Calculation

We can solve for peak gait events based on the learned gait model:

$$\hat{y}_t = \sum_{m=0}^{M} (\alpha_{t,m} \cos(m\phi_t) + \beta_{t,m} \sin(m\phi_t)) \tag{A.1}$$

Since we are interested in peaks, we find ϕ such that the derivative is equal to 0. Simplifying for the derivative of the gait model with respect to ϕ, we get:

$$\frac{d\hat{y}_t}{d\phi_t} = \sum_{m=0}^{M} (-m\alpha_{t,m} \sin(m\phi_t) + m\beta_{t,m} \cos(m\phi_t)) \tag{A.2}$$

$$\frac{d\hat{y}_t}{d\phi_t} = \sum_{m=0}^{M} (jm\alpha_{t,m}(\frac{e^{jm\phi_t} - e^{-jm\phi_t}}{2}) + m\beta_{t,m}(\frac{e^{jm\phi_t} + e^{-jm\phi_t}}{2}) \tag{A.3}$$

$$\frac{d\hat{y}_t}{d\phi_t} = \sum_{m=0}^{M} \frac{m}{2}[(\beta_{t,m} + j\alpha_{t,m})e^{jm\phi_t} + (\beta_{t,m} - j\alpha_{t,m})e^{-jm\phi_t}] \tag{A.4}$$

For $\frac{d\hat{y}_t}{d\phi_t} = 0 \longrightarrow 2e^{jM\phi_t}\frac{d\hat{y}_t}{d\phi_t} = 0$, therefore

$$\sum_{m=0}^{M} m[(\beta_{t,m} + j\alpha_{t,m})e^{j(m+M)\phi_t} + (\beta_{t,m} - j\alpha_{t,m})e^{j(M-m)\phi_t}] = 0 \tag{A.5}$$

Letting $x = e^{j\phi_t}$,

$$\sum_{m=0}^{M} m[(\beta_{t,m} + j\alpha_{t,m})x^{m+M} + (\beta_{t,m} - j\alpha_{t,m})x^{M-m}] = 0 \tag{A.6}$$

We can solve for the roots of the left hand side of the equation, *i.e.* the values of x which satisfy the equation, using a solver in MATLAB. We can then use these values of x to solve for ϕ which causes the derivative of the analytical model to be zero (*i.e.* peaks and troughs) by setting $\phi = \angle x$. Finally, we assign ϕ which gives the highest $\hat{y}_t$ as the peak phase. Each time this phase value is passed, we identify a peak event.